PALEOBURIAL, HYDROCARBON GENERATION, AND MIGRATION IN THE CÓRDOBA PLATFORM AND VERACRUZ BASIN: INSIGHTS FROM FLUID INCLUSION STUDIES AND TWO-DIMENSIONAL (2D) BASIN MODELING

ESMERALDA GONZALEZ
Pemex Exploration and Production, Veracruz, Mexico and Direction Géologie–Géochimie–Géophysique, IFP Energies nouvelles, 1–4 Avenue de Bois-Préau, F-92852 Rueil-Malmaison Cedex, France

HELGA FERKET
Direction Géologie–Géochimie–Géophysique, IFP Energies nouvelles, 1–4 Avenue de Bois-Préau, F-92852 Rueil-Malmaison Cedex, France and Mexican Petroleum Institute (MPI), Mexico DF, Mexico and VITO, Boeretang 200, 2400 Mol, Belgium

JEAN-PAUL CALLOT*
Direction Géologie–Géochimie–Géophysique, IFP Energies nouvelles, 1–4 Avenue de Bois-Préau, F-92852 Rueil-Malmaison Cedex, France. Present address: UMR CNRS TOTAL 5150 "Laboratoire des Fluides Complexes et leurs Réservoirs," Université de Pau et des Pays de l'Adour I.P.R.A. Avenue de l'Université BP 1155 64013 PAU Cedex, France
e-mail: jean-paul.callot@univ-pau.fr

NICOLE GUILHAUMOU
MNHN, Muséum National d'Histoire Naturelle, Laboratoire d'étude de la matière extra-terrestre, 57 rue Cuvier, F-75005 Paris, France

SALVADOR ORTUNO
Mexican Petroleum Institute (MPI), Mexico DF, Mexico

AND

FRANÇOIS ROURE
Direction Géologie–Géochimie–Géophysique, IFP Energies nouvelles, 1–4 Avenue de Bois-Préau, F-92852 Rueil-Malmaison Cedex, France and Vrije Universiteit Amsterdam, The Netherlands

Abstract: One-dimensional and two-dimensional basin modeling has been performed along a regional transect crossing the Córdoba Platform allochthons and the autochthonous Veracruz Basin in order to infer the burial and kinematic evolution and to determine timing of hydrocarbon migration and charge in this famous Mexican petroleum province. Vitrinite reflectance, Rock-Eval data, and bottom-hole temperatures have been used to calibrate the heat flow and thermal evolution of the Veracruz Basin, where no erosion occurred.

The Córdoba Platform and Veracruz Basin in Eastern Mexico comprise the southernmost extent of the Laramide foreland fold-and-thrust belt, which developed along the eastern border of the North American Cordillera from Late Cretaceous to Eocene. Unlike in the Canadian Rockies, where pre-orogenic strata are relatively isopachous, this segment of the North American craton has been strongly affected by the Jurassic rifting and opening of the Gulf of Mexico. Substantial thickness and facies changes between horsts and grabens control the lateral and vertical distribution of Mesozoic source rocks and hydrocarbon reservoirs.

In the east, thick Paleogene and Neogene sequences in the Cordilleran foreland provide a continuous sedimentary record in the Veracruz Basin. In the west, however, the Middle Cretaceous carbonates of the Córdoba Platform generally constitute the main outcropping horizon in the adjacent thrust belt, making it difficult to reconstruct its burial evolution from the Laramide orogeny onward.

Cemented veins were sampled in reservoir intervals of the thrust belt. Petrography, stable isotope analyses, and fluid inclusion studies (microthermetry, Synchroton Fourier Transform Infra-Red analyses) on these samples revealed the diagenetic history of the reservoirs. Where diagenetic phases could be constrained in time and with respect to the tectonic evolution, fluid inclusion temperatures provide an additional paleothermometer in areas where major erosion occurred. Pressure–temperature modeling of simultaneously entrapped aqueous and oil-bearing inclusions indicates more than 4.5 km of erosion of Late Cretaceous–Paleocene sequences in the thrust belt, which can be accommodated in palinspastic sections only by restoring a hypothetical foredeep basin. This implies that the current east-dipping attitude of the basement beneath the Córdoba Platform developed after Laramide deformation, accounting for a major change in paleofluid dynamics. Fluid flow and basin modeling of the Veracruz section has been performed using CERES2D to infer the paleofluid dynamic associated with the petroleum system evolution. Following the initial phase of geometric model building and calibration against the thermal and burial history inferred, the modeling accounted for the past migration pathways for both water and oil and gas fluids. Unlike in most other foreland fold-and-thrust belts, hydrocarbons generated in Jurassic source rocks from the Veracruz foreland are currently migrating westward toward the thrust belt, accounting for a post-Laramide charge of the frontal duplexes of the Cordilleran thrust belt.

Key words: Veracruz Basin, fluid inclusion, basin modeling, CERES2D

Analyzing the Thermal History of Sedimentary Basins: Methods and Case Studies
SEPM Special Publication No. 103, Copyright © 2012
SEPM (Society for Sedimentary Geology), ISBN Print ISBN 978-1-56576-315-9, CD/DVD ISBN 978-1-56576-317-3, p. 167–186.

INTRODUCTION

In the scope of the Sub-Thrust Reservoir Appraisal (SUBTRAP) project (e.g., Roure et al. 2005, 2010), IFP New Energies (formerly IFP) and the Mexican Petroleum Institute (IMP) initiated a long-term collaborative study of fluid–rock interactions and reservoir quality prediction in Cretaceous carbonates of the Córdoba Platform in Eastern Mexico. This area constitutes the southernmost extent of the Laramide thrust front and can be traced along the eastern edge of the North American Cordillera, from Canada in the north to the Gulf of Mexico in the south (Fig. 1). This study identified numerous episodes of pressure–solution fracturation and hydraulic brecciation in the platform carbonates related to increasing burial and tectonic stress (layer parallel shortening), as well as exposure events and coeval paleokarst development (Ferket et al. 2000, 2003, 2004, 2006; Ferket 2004, 2006). During the first phase of the SUBTRAP project, two-dimensional (2D) basin modeling was also performed to reconstruct the paleoburial history of individual reservoir and source rock horizons using the software Thrustpack (Divies and Sassi 1996; Sassi and Rudkiewicz 1999, 2000). This modeling coupled kinematic evolution of the thrust belt with erosion and deposition of synorogenic sediments. The modeling was also applied to reconstruct the structural evolution of three regional sections extending from the Cordilleran foothills in the west to the Veracruz Basin in the east from their Middle Cretaceous pre-orogenic configuration until present day (Ortuño et al. 1999, 2003). The Thrustpack modeling enabled us to (1) reconstruct the thermal evolution of these cross sections using bottom-hole temperature (BHT) data and maturity ranks of the organic matter (i.e., vitrinite reflectance [R_o] and Rock-Eval [T_{max}]) for calibration and (2) simulate the maturity evolution of source rocks from the Late Jurassic onward. These preliminary models and current petroleum occurrences indicate that a petroleum charge was generated in the adjacent Veracruz Basin (Figs. 1, 2) during post-Laramide subsidence, which migrated westward, filling traps in frontal duplexes of the Cordilleran thrust belt.

This article summarizes results from the second phase of the SUBTRAP project, which focused on remaining uncertainties relating to (1) the past attitude of the basement, (2) the timing and amount of exhumation and unroofing of the foothills, and (3) the timing and pathways of regional fluid flow and hydrocarbon migration. Following a short summary of the regional geology and current understanding of the petroleum systems, the article focuses on fluid inclusion (FI) studies that were employed to better constrain estimates of the eroded thicknesses. Fluid inclusion analysis is a paleothermo-barometer that is independent of the other thermal calibrations, which are based on

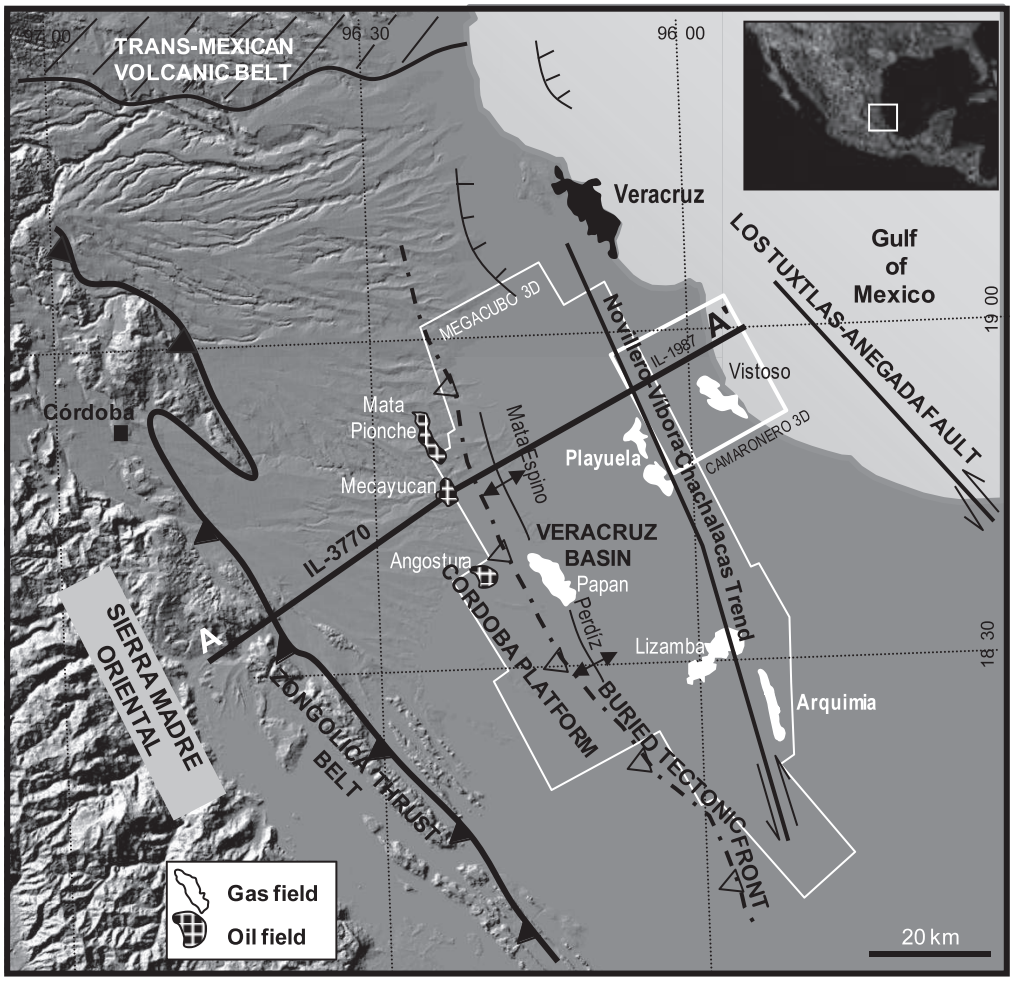

FIG. 1.—Location map of the Veracruz Basin, Córdoba Platform, and Zongolica thrust belt, outlining as well the main oil and gas fields of the platform. AA′ indicates the trace of the modeled transect.

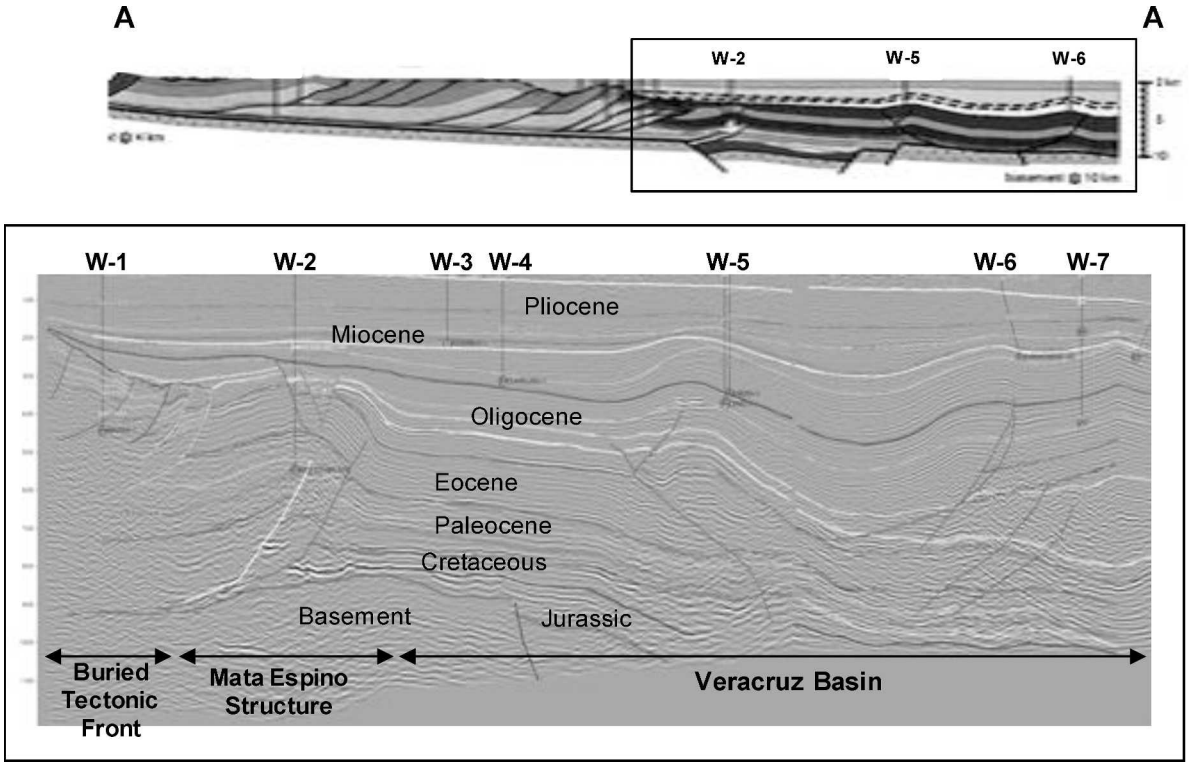

FIG. 2.—Top: Structural section AA'. Bottom: Seismic profile imaging the transition between the Córdoba Platform and thin-skinned Laramide thrust front in the west and basement-involving inverted structures of the Veracruz Basin in the east.

organic matter maturity ranks (see Roure et al. 2010). A direct consequence of the FI study was to provide more realistic control on the paleoburial of the Cretaceous platform carbonates and on the former configuration of the underlying basement. Subsequently, we used the inferred structural evolution of an existing regional cross section as input data for a basin modeling experiment using the CERES2D software, a dedicated basin modeling tool, developed for tectonically complex areas (see Appendix). This software was used to simulate the regional fluid flow evolution and hydrocarbon migration.

GEOLOGICAL SETTING AND CURRENT KNOWLEDGE OF THE PETROLEUM SYSTEMS OF THE CÓRDOBA PLATFORM AND VERACRUZ BASIN

The Córdoba Platform is located south of the Trans-Mexican volcanic axis (Fig. 1) and belongs to the Zongolica thrust belt (Ortuño 1991; Meneses-Rocha et al. 1997; Ortuño et al. 1999, 2003; Rojas 1999; Fig. 2). The Córdoba Platform is predominantly made up of Cretaceous carbonates and constitutes the southernmost portion of the Laramide thrust belt system. This thrust belt developed along the eastern edge of the North American Cordillera during Late Cretaceous to Eocene, from the Canadian Rockies in the north to the Sierra Madre Oriental in Mexico in the south (Fig. 1). To the east, the foreland autochthon consists of the Veracruz Basin (Fig. 1), where thick Oligocene and Neogene siliciclastics derived from post-Laramide erosion of the thrust belt accumulated (Jennette et al. 2003a, 2003b). A short summary of the geodynamic and paleogeographic evolution, lithostratigraphy, and petroleum systems of this onshore part of Eastern Mexico is provided below.

Geodynamic Evolution of Eastern Mexico

The tectonic evolution of eastern Mexico is directly linked to the history of the Gulf of Mexico. The Jurassic events that eventually formed the Gulf of Mexico began with a rifting episode during Late Triassic to Jurassic, leading to continental break up and progressive oceanic accretion between the Maya block in the west and the actual North American Platform (Campa and Coney 1983, Salvador 1991, Pindell 1994). At the western margin of the Gulf of Mexico, rift-related crustal thinning resulted in the formation of two basins: the Veracruz Basin in the east and the Zongolica Basin in the west (not shown). In these basins, euxinic conditions and source rock deposition prevailed during the Late Jurassic. These two domains were still characterized by pelagic carbonate sedimentation during Cretaceous episodes of post-rift thermal subsidence, whereas the intervening Córdoba Platform, comprised of ancient horsts, was characterized by shallow-water sedimentation during the Early and Middle Cretaceous. Cordilleran deformation was first recorded in the study area by local uplift and karstification of the carbonate platform during the Campanian in response to tectonic loading of the hinterland. A foredeep with calcareous flysch deposition formed between the forebulge and the tectonic front at that time. Platform exposure was followed by drowning of ancient platform domains and onset of Maastrichtian deep-water clastic sedimentation in the various units of the Zongolica thrust belt. These events thus record a short episode of foreland flexuration.

During the Late Cretaceous and Paleocene, the Mesozoic series of the Zongolica Basin and Córdoba Platform were tectonically detached from their crystalline basement and thrusted eastward toward the autochthonous foreland. The thrust front was located at the former platform-to-basin transition, where major deformation of carbonaceous

sediments and stacking of numerous duplexes occurred. These duplexes formed traps for major oil pools in Middle and Upper Cretaceous carbonate reservoirs (Fig. 2; Roure 2008). Thrusting resulted in a rapid exhumation and unroofing of the Mesozoic carbonate units, with a massive supply of clastic material toward the still-subsiding Veracruz Basin.

Basement faults of the Veracruz Basin were ultimately reactivated by transpression during the Late Miocene, resulting in the development of wide anticlinal traps, such as the Novillero–Vibora–Chachalacas (NVC) anticline and the NW-trending Mata Espino and Perdiz structures (Fig. 1), where biogenic gas accumulations occur in Neogene sandstone reservoirs (Espinoza and Toriz 2005).

Lithostratigraphic Description

Pre-Rift and Syn-Rift Sequences: The crystalline basement of the Córdoba Platform and Veracruz Basin is made up of Permo-Triassic metamorphic rocks (Jacobo 1986). In the former basinal domains, the basement is overlain by Triassic–Jurassic (?) continental red beds of the Cahuasas and Rosario formations (Figs. 2, 3).

Passive Margin Sequence: Late Jurassic calcareous black shales of the Tepexilotla Formation (Figs. 2, 3) crop out along the exposure of the sole thrust of the Sierra de Zongolica in the west and have been drilled in one well in the southern part of the Veracruz Basin. The thickness of these rocks measures approximately 250 m (Vázquez 2004).

Overlying Cretaceous sediments comprise a succession of limestones (mudstones to grainstones) that display drastic lateral thickness and facies variations between platform and basinal domains. The Lower Cretaceous interval is 1000 to 1500 m thick and consists of partially dolomitized micritic limestones typical of a lagoonal environment. These rocks grade upward into dolomites and partially dolomitized limestone with evaporate intercalations. The overlying Middle Cretaceous Orizaba Formation is 1500 to 2000 m thick in the central and western parts of the platform (Ferket 2004) but gradually thins to the east. In the SW portion of the platform, the basal units of this formation consist of dolomites and evaporites, which commonly form decollement horizons during Laramide deformation. The lower and middle parts of the Orizaba Formation are partly dolomitized, while the upper part is dominated by light-gray, miliolid-rich, bioclastic limestone.

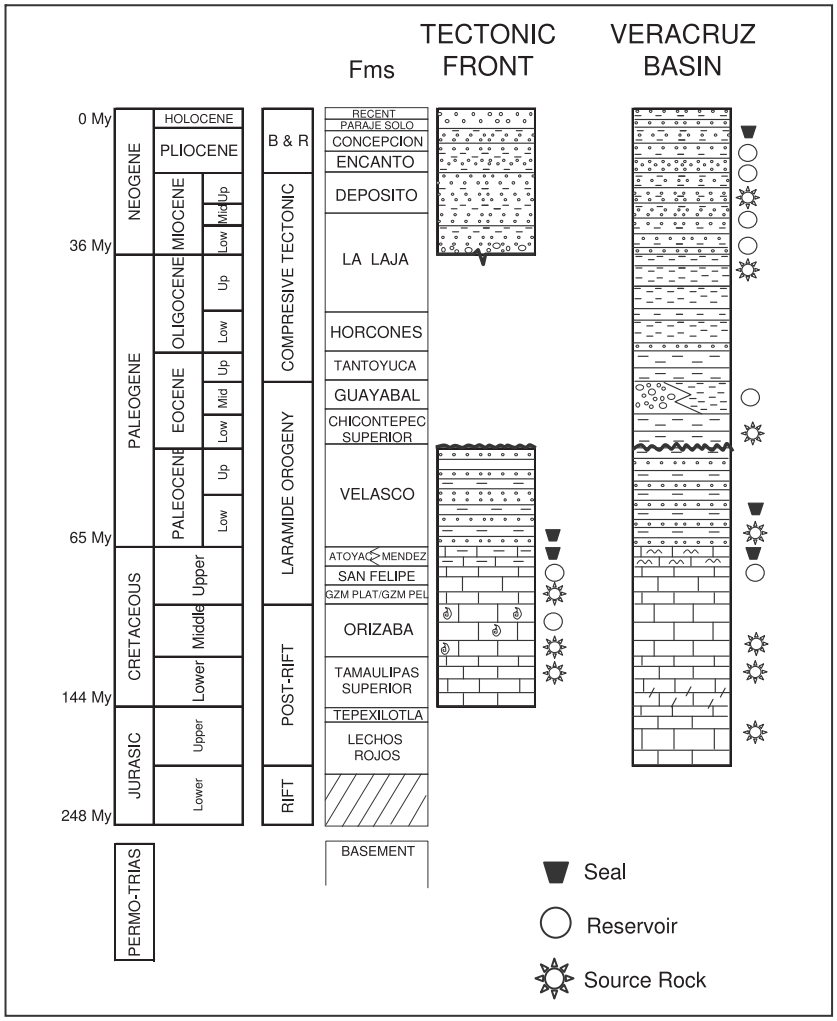

FIG. 3.—Stratigraphic column for the Córdoba Platform and Veracruz Basin, showing potential source rock, reservoir, and seal horizons.

The Upper Cretaceous sequence is divided in five formations, some of which are coeval but which record different paleo-environments. The Guzmantla Formation is 1500 m thick and comprises Lower Turonian and Upper Coniacian–Santonian units (Figs. 2, 3). The lower unit (Guzmantla "pelagica") is composed of well-bedded argillaceous limestones deposited during a maximum flooding phase. The upper unit consists of partly dolomitized limestone, typical of an inner platform with isolated reefs, shoals, and lagoons. The Maltrata Formation is 100 to 400 m thick, consists of argillaceous limestones deposited in deeper anoxic water around the platform, and is considered to be time-equivalent to the lower Guzmantla Formation.

In the Zongolica belt, the Campanian is represented by a depositional hiatus and local paleokarst development; i.e., subaerial exposure. At the same time along the eastern platform edge, slope breccias and intercalated pelagic limestones of the San Felipe Formation were deposited. The Atoyac Formation of Maastrichtian age overlies the Campanian unconformity only in the easternmost outcrops of the Zongolica thrust belt and constitutes the last platform sedimentation in the area. No complete section of the Atoyac Formation has been preserved as a result of post-Laramide erosion, leaving only minimum estimates of the original thickness (300–400 m). The Upper Cretaceous Méndez Formation comprises deep-water shaly limestones (Ferket 2004) that are believed to have originally covered the whole passive margin, but their residual thickness after erosion locally amounts to a maximum of 300 m.

Laramide Flexural Sequence: Erosional remnants in the Zongolica foothills are preserved in a sequence of Laramide-age Late Cretaceous and Paleocene siliciclastic turbidites, and few well records are available with which to document the Paleocene lithofacies in the adjacent Veracruz Basin (Berman et al. 1995).

In contrast, the Eocene sequence of the Veracruz Basin is represented by up to 1400 m of conglomerate, sandstone, and shale derived from the erosion of the Laramide thrust belt (Figs. 2, 3). Seismic and well data indicate that near-source debris-flow sediments close to the tectonic front grade into thick packages of turbidites in the basin, resulting in a basinward thickening of the sequence (Jennette et al. 2003a, 2003b).

Post-Laramide Sequences: Outcrops and wells provide direct control on Oligocene lithofacies in the Veracruz Basin. Nevertheless, interpretations of lithologies and depositional systems are largely based on seismic data. In a few locations where the Oligocene has been drilled it consists of fine sediments deposited in deep-water environments.

The Miocene series unconformably overlies the Oligocene. Lower Miocene is made up of conglomerates with subordinate beds of sandstone and shales that constitutes the upper part of the La Laja Formation (Figs. 2, 3). These sediments were probably transported through large submarine canyons that served as important conduits for the transport of erosional products from the thrust belt to the Gulf of Mexico (Berman et al. 1995). In the Middle Miocene, the basin was still fed through a complex of channels, also filling the former canyons created during the Early Miocene. During the Late Miocene (Depósito Formation; Fig. 3), uplifted and eroded areas to the NW and SW of the Córdoba Platform continued to feed basin-floor fans and complex channel systems that carried a great quantity of sand and mud toward the basin. Simultaneously, during the Late Miocene, reactivation of basement faults in the Veracruz Basin resulted in strata onlapping onto the flanks of localized antiforms, accounting for a number of stratigraphic traps that host major gas fields (e.g., Arquimia field located along the southeastern flank of the NVC structure; Fig. 1).

The Pliocene sequence consists of clayey–sandy sediments of the Encanto and Depósito formations (Fig. 3) that onlap a gently eastward-dipping erosional surface in the foothills (Fig. 2) and rapidly thickens east of the thrust front. Its overall thickness varies from 1000 m near the thrust front in the west to 2000 m or more in the southeastern part of the Veracruz Basin. Large clinoforms prograde to the southeast and have their principal supply source in the northwest. They contribute to form great submarine fans constituted by a complex of interbedded channels. Sandstone layers of Lower Pliocene form clinoforms that host important gas fields in the Veracruz Basin (e.g., Lleida field situated north of Veracruz; Fig. 1).

TABLE 1.—Source rock data of petroleum system in Veracruz Basin (Gonzalez-Mercado 2007).

	Upper Jurassic	Lower and Middle Cretaceous	Upper Cretaceous	Paleocene to Miocene
Kerogen	II	II	II	III
TOC (%)	2	3.50	2	1
IH	475	511–531	300–600	
S_2 (mg HC/g)	2.12	7.5 and 10.3	7.36	
T_{max} (° C)	>450	426–470	410–434	

TOC = total organic compound; IH = hydrogen index; S2 = second peak during Rock-Eval pyrolysis; Tmax = maximal temperature at S2 peak.

Current Knowledge on the Petroleum Systems in the Córdoba Platform and Veracruz Basin

The pattern of oil and bitumen occurrences indicates that two petroleum systems are present (Guzman-Vega et al. 2001, Prost and Aranda-Garcia 2001). The first of these includes bitumen and heavy oil in Cretaceous platform carbonates of the Cordillera allochthon: for example, the Peñuela quarry near the city of Córdoba. These hydrocarbon accumulations are believed to record early petroleum migration and trapping, followed by biodegradation in anticlines that formed in the Paleogene, and are located quite far from the productive oil fields of the frontal duplexes. Ferket et al. (2010) suggested that oil shows near the city of Córdoba are related to short vertical migration from undocumented intraplatform, organic-rich sediments. Another possibility for these oil occurrences is a longer-range eastward migration from the Jurassic source rocks of the former Zongolica Basin. This should have occurred prior to thrusting and unroofing of this basinal domain eastward on top of the Córdoba Platform.

Oil fields in the frontal complexes are almost certainly related to a different petroleum system, directly associated with the Veracruz Basin (Guzman-Vega et al. 2001). Only this latter petroleum system is discussed further in this article.

Source Rocks: Source rocks associated with hydrocarbons in the frontal complexes include the Upper Jurassic Tepexilotla Formation, Lower Cretaceous Tamaulipas Superior Formation, and Middle Cretaceous Orizaba Formation (Vázquez 2004, 2008) and intervals in the Paleocene to Miocene section. Details regarding source rock quality, character, and interpretation are provided in Table 1.

a. The Upper Jurassic (Tithonian) is the principal source rock (Vázquez 2004) and consists of shaly limestones of the Tepexilotla Formation. The net thickness of the source interval is about 150 m (Vázquez 2004). The organic matter is algal-derived Type II kerogen, with total organic carbon (TOC) content averaging 2% (Guzman-Vega et al. 2001); a hydrocarbon index (HI) of 475; S_2 of 2.12 mg hydrocarbons (HC)/g rock, and a T_{max} of >450° C. These analyses correspond to mature source rocks; the original TOC for Jurassic source rocks is 3.5 to 4% (Vázquez 2008). Biomarker

analyses on Jurassic oils indicate a calcareous marine siliciclastic environment (Berman et al. 1995).

b. Middle and Lower Cretaceous argillaceous and evaporitic limestones also are considered to be source rocks for liquid and gas hydrocarbons (Vázquez 2004). The net thickness of the source interval is 130 m. Pyrolysis and organic petrography indicate a mean TOC value of 3.5% (Guzman-Vega et al. 2001), Type II kerogen, an HI ranging from 511 to 531, S_2 between 7.5 and 10.3 mg HC/g rock, and T_{max} values between 426 and 470° C. These parameters correspond to a relatively immature rock and represent good source rock potential (Vázquez 2008). Biomarkers on such oils point out a calcareous–evaporitic marine family.

c. The Upper Cretaceous (Turonian) contains argillaceous limestones with a net generative thickness ranging from 50 to 80 m. According to Vázquez (2004), the average TOC value is 2%; HI is 300 to 600; S_2 is 7.36 mg HC/g rock, and T_{max} ranges from 410 to 434° C. The kerogen is Type II, and biomarkers indicate an anoxic calcareous marine source rock.

d. Some units within the Paleocene to Miocene sequence have been characterized as source rocks for biogenic gas based on Rock-Eval analyses. Their kerogen is Type III, and TOC amounts to 1% (Vázquez 2008). The next table summarizes the source rock parameters.

A consequence of the geologic complexity of the Veracruz Basin is that the same source rocks can present different degrees of maturity. Thus, according to Table 1, the T_{max} of the Upper Jurassic rocks from the basin depocenter indicates that this source rock is currently overmature, while the same rocks located along the Zongolica thrust belt (Fig. 1) are still into the oil generation window.

According to their T_{max} data, the Middle and Lower Cretaceous source rocks are currently within the window of generation, in contrast to the Upper Cretaceous source rock from the Platform of Córdoba, which is currently immature.

At the moment, for the Tertiary source rocks (Paleocene and Eocene) located in the Veracruz Basin, thermal conditions for oil generation are present; however, the organic matter contained in these rocks is Type III, which generates gas.

Reservoirs: Oil reservoirs in the Córdoba Platform are hosted in limestone and dolomites of the Middle Cretaceous Orizaba Formation, as well as in limestone of the Upper Cretaceous Guzmantla and San Felipe formations (Berman et al. 1995). Some limestones within the Guzmantla and San Felipe formations exhibit breccia textures. The Middle and Upper Cretaceous reservoirs are characterized by dual porosity–permeability systems, with contributions from both matrix and fracture porosity.

Hydrocarbon production in the Veracruz Basin is mainly thermogenic and biogenic gas trapped in clastics sequences throughout the entire Miocene and in the Lower Pliocene (Vázquez 2008). The only oil field in the Veracruz Basin is located in conglomerates of Eocene age (Geologic report of well Perdíz-1, unpublished data, 2000).

Seals: The main seals for reservoirs located in duplexes at the Laramide tectonic front are the Upper Cretaceous Méndez Formation and the Paleocene shales of the Velasco Formation (Fig. 3). Reverse faults form efficient lateral seals (Espinoza and Toriz 2005; Fig. 2). In the Veracruz Basin, the seals are essentially Pliocene shale varying from 100 m thick near the thrust front to 2500 m thick in the eastern part of Veracruz Basin (AIV-Pemex 2007, 2010).

Timing of Hydrocarbon Generation, Migration, and Trapping: Organic geochemistry data such as biomarkers and diamandoids (Vázquez 2004, 2008) indicate multiple sources and migration pathways, revealing a complicated petroleum system. At least two hydrocarbon migration episodes of oils of differing maturity were recorded in Cretaceous reservoirs at the buried tectonic front. Oil migration occurred westward from sources in the foreland toward the thrust belt and is generally believed to have occurred mainly from the Miocene onward (e.g., Ortuño et al. 2003 [and references therein]). Two types of gases are observed in the oil fields located in the thrust belt cretaceous rocks. The first type of gas is found in association with oil, whereas the second one is a more evolved dry gas, identified through isotopic analysis, chromatography, and biomarker analysis. We propose that both gases come from the same source rock, the evolved gas originating from a second phase of maturation, probably after the source rock was affected by the buried caused by the Laramide Orogeny. Gases in the Veracruz Basin often represent mixtures between thermogenic and biogenic gases (Vázquez 2004, 2008), but because direct evidence concerning the timing and identification of migration pathways is lacking, basin modeling is required.

TABLE 2.—Tectonic events and associated heat flow data used for the thermal field modeling (Gonzalez-Mercado 2007).

Age	Stage	Tectonic event	Heat flow
416	crustal part	pre-rift	65
248	basement		60
144.2	Jurassic	rift	55
112.2	Early Cretaceous		50
93.5	Middle Cretaceous	post-rift	50
83.5	Santonian		50
65	Maastrichtian	Laramide stage	50
50	Early Paeocene		50
41.3	Upper Paleocene to lower Eocene		50
37.1	Middle Eocene		47
33.8	Upper Eocene	main phase of shortening	35
24.3	Oligocene		30
16.4	Lower Miocene		30
11.7	Middle Miocene		30
5.7	Upper Miocene		30
0	Pliocene to present day	basin and range stage	30

CONSTRUCTION OF THE STRUCTURAL SECTION AND QUANTIFICATION OF ERODED THICKNESSES

Present-Day Structural Section

The 120-km-long section is located in the north of Veracruz. It extends NE–SW from the Tezonapa-1 well at the western edge of the section, to the Tortuguilla-1 well in the east of the Veracruz Basin (Fig. 1). From west to east the section includes the Zongolica thrust belt; the buried, folded Cordoba Platform; and the Veracruz Basin (Fig. 2). Seismic data are lacking for the western part of the modeled section (Córdoba Platform). Structural interpretations and reconstructions in this area are therefore derived from field observations and available well data. In the eastern part of the Veracruz Basin, data from two three-dimensional (3D) seismic volumes were available to reconstruct the transect (Figs. 1, 2). Calibration data along the entire transect were provided by a large number of exploration wells.

Fluid Inclusion Data, PVT Modeling, and Paleoburial Estimates

The amount of erosion of platform carbonates in the thrust belt was first estimated based on platform reconstructions and thickness variations of the carbonate formations throughout the platform and basin, as recorded in several exploration wells (Ferket 2004, 2006). This exercise was relatively straightforward for the Orizaba and Guzmantla formations but much more ambiguous for laterally restricted formations, such as the Atoyac, Maltrata, and San Felipe formations. Nevertheless, the latter formations are thin compared to the main platform formations, and possible errors in estimates of their original thicknesses therefore do not engender significant errors in reconstructing paleoburial and erosion.

In order to further estimate paleoburial depths and amount of erosion in the thrust belt zone, where several stratigraphic sequences have been stacked and where syntectonic flysch has accumulated in basins, several generations of crosscutting veins were studied from outcrops and exploration wells. As much as possible, these diagenetic phases were placed in a relative timescale and, where possible, also in an absolute timescale. Some minerals contain fluid inclusions that captured relics of ancient formation fluids. Microthermometric study of fluid inclusions gives information on paleotemperature and composition of the fluids preserved in them. The measured homogenization temperatures (Th) give minimum trapping temperatures. In order to determine the real trapping conditions, a pressure correction is needed. In some cases paleopressures can be calculated or estimated from crosscutting relationships between the water isochors and an independent paleothermometer or from cogenetic aqueous and hydrocarbon-filled fluid inclusions. Furthermore, it is not always clear whether a fluid inclusion formed from a fluid in equilibrium with the host rock, from a hydrothermal fluid at higher temperature, or from a cooler fluid. Although exact temperature values might not be available, the diagenetic events and minimum temperatures can be valuable in unraveling the burial history of complex areas.

A data set with useful diagenetic markers has been compiled over the last 12 years for the Córdoba–Veracruz area. The vein filling minerals have been characterized by petrography, stable oxygen and carbon isotopes and Sr isotope analyses, microstructural characteristics, and fluid inclusion data. When fluid inclusion characteristics, such as vapor:liquid ratio and Th-Tm spreads, show relatively homogeneous populations, then it is reasonable to assume that the fluids were in thermal equilibrium with the host rock. Any fluid inclusion population representing either necking down, extreme variation in Th, or variable characteristics that could not be assigned to a specific generation was left out of the data set. Under these conditions one can use the Th values as control points on the burial curve to test kinematic scenarios, always keeping in mind that they represent minimum trapping temperatures. Depending on the isochors (composition), the needed correction is expected to be smaller or higher. In the Córdoba area, fluid inclusions were studied in several minerals (dolomite, fluorite, quartz, and calcite) that precipitated during the burial history before, coeval with, and after hydrocarbon migration, from two Mesozoic levels: the Orizaba and Guzmanta formations (Ferket 2006, Ferket et al. 2010; Figs. 4, 5).

The information inferred from the fluid inclusion data set (Pressure and Temperature of entrapment) was used to calibrate one-dimensional (1D) basin modeling. In two cases, fluid inclusions provided crucial information that could be used to calculate the amount of burial. Quartz–cement in dolomites of the Orizaba Formation hosted four different generations of water–hydrocarbon fluid inclusions (both mixed water and hydrocarbon fluid inclusions, and water-free fluid inclusions). The first two generations are cogenetic primary water–hydrocarbon fluid inclusions, and there are also two sets of secondary fluid inclusions (Fig. 4). In this case, a combination of microthermometric and Synchroton Fourier Transform Infra-Red analyses (SFTIR; see Guilhaumou and Dumas 2005 for explanation) enabled us to perform Pressure and Temperature (PT)-modeling and to calculate paleopressures (Ferket et al. 2010; Fig. 4). These techniques are described in detail in Ferket et al. (2010). The isochors for the hydrocarbon phase were constructed in a PT diagram based on modeling of the progressive volume changes of the vapor bubble in the hydrocarbon fluid inclusion during heating (Fig. 6) and based on the SFTIR results (see Guilhaumou et al. 2004 for explanation). Combination of these isochors with the water isochors gives an estimate of the real trapping pressure. Elsewhere, calcite cement in limestone from the Guzmantla Formation at the Peñuela paleoseep (Ferket et al. 2003, 2010; Fig. 5) appeared to contain pure-oil fluid inclusions. This points to an already-differentiated reservoir with well-individualized water, oil, and gas levels, rather than to primary hydrocarbon migration. Pressure and Temperature (PT)-modeling of these fluid inclusions (Fig. 5) also gave minimum estimates for the paleopressure.

Based on these two cases, it could be derived that an original Late Cretaceous to Paleocene flysch cover of at least 4.5 km must have been present in the western part of the Córdoba Platform. This is particularly well expressed from the modeled fluid inclusion for the Orizaba Formation, with an entrapment pressure of more than 250 bars (Fig. 4). Thermal maturity (T_{max}) in the Córdoba area (Ferket et al. 2006) also fits this kinematic evolution, even better than do the classical burial scenarios (Fig. 7). This thickness of eroded sediments should have been present originally on top of the Peñuela paleoseep, which is situated in an upper thrust sheet. This degree of missing section cannot be explained by tectonic loading on top of this thrust unit and cannot be restored in kinematic reconstructions. Such deposition can only be explained by the development of a local foredeep that received erosional products of the Zongolica thrust belt (Ferket et al. 2010). This foredeep developed just after a short episode of foreland flexuring, documented by uplift and local karstification of the carbonate platform (forebulge) during the Late Cretaceous. A minor portion of the calculated 4.5-km overburden may also have been related to tectonic stacking (assuming an extension of the allochthonous nappes with relics of the former Zongolica Basin eastward for more than 16 km).

TWO-DIMENSIONAL RECONSTRUCTION OF INTERMEDIATE GEOMETRIES AND PALEOBURIAL: TOWARD A KINEMATIC SCENARIO

Starting from the present-day structural section, a back-stripping restoration of all lithostratigraphic units was carried out that accounted for paleobathymetry, deformation, erosion, and compaction. The geologic concepts for this restoration were taken from SUBTRAP (Ortuño et al. 1999, 2003) and Ferket (2006). A summary of the main kinematic steps is given below.

Paleozoic to Early Cretaceous

The oldest rocks of the section correspond to crystalline basement of Paleozoic–Triassic age (radiometric ages of 248.2 Ma; Pemex-Schlumberger 2000), partly eroded during the pre-rift period. The first tectonic episode relates to Late Jurassic rifting and opening of the Gulf of Mexico. During the Upper Jurassic, continental red beds as well as marine calcareous sediments and clays (Tithonian source rocks) were deposited in half-graben structures. The subsequent Early Cretaceous post-rift stage is marked by regional carbonate sedimentation in platform and basin domains on former horsts and grabens (Fig. 8a).

Albian–Cenomanian

This stage corresponds to the principal development of the Córdoba Platform, characterized by thick accumulation of bioclastic limestone.

Cement phase	Petrography	Stable isotopes (‰PDB)	FI	Interpretation
Dolomite D	Zoned with cloudy core and transparent rims; in (breccia-) veins; CL: dull red luminescent	$\delta^{18}O$ -3.5 to -6.0 $\delta^{13}C$ +3.7 to +0.2	Primary FI H_2O-NaCl T_h (center) 50-60°C T_h (rim) 70-80°C	Burial cement
Fluorite F	Cubic crystals with a bitumen-coating on free faces, often corroded before precipitation of calcite; in (breccia-) veins; CL: extinguishing blue to non-luminescence		Secondary FI Non-fluorescent H_2O-NaCl T_h 110-155°C T_m -5.7 to -9.1°C	Hot saline fluid preceding HC trapping in reservoirs i.e. peak Laramide burial
Quartz Q	Euhedral cement in breccia vein, postdating D and F and preceding C1, intergrown with solid bitumen and containing blue fluorescent H_2O – hydrocarbon (HC) FI		Primary FI i) HC-(H_2O) T_h 90-105°C 35-40mol% CH_4 C7-C8 alkane equivalent ii) H_2O-NaCl-(CH_4-HC) T_h 140-150°C T_m -8.1 to -8.3°C Secondary FI iii) HC T_h 75-85°C 35-55mol% CH_4 C6-C7 alkane equivalent iv) H_2O-NaCl T_h 70-80°C T_m -0.6 to -1.7°C	Trapping and early post-trapping conditions at high temperature and pressure (200 bar < P < 350 bar), i.e. peak Laramide burial Intergrown bitumen relates to thermochemical sulfate reduction (TSR)
Calcite C1	Replacive after anhydrite, neomorphic, megacrystals after corrosion phase; associated with sulfides and pyrobitumen; CL: non-luminescent	$\delta^{18}O$ -16.7 to -5.0 $\delta^{13}C$ -18.0 to -2.5	At least partly secondary H_2O-NaCl T_h 71-110°C and 45-75°C T_m -3.3 to +0.0°C	Related to thermochemical sulfate reduction (TSR)
Calcite C2	Common cement phase in veins; after corrosion phase; CL: sector-zoned dull luminescent	$\delta^{18}O$ -11.9 to -3.5 $\delta^{13}C$ -2.4 to +1.9	Primary FI H_2O-NaCl T_h 45-66°C T_m ~0.0°C	Post-Laramide denudation and cooling phase

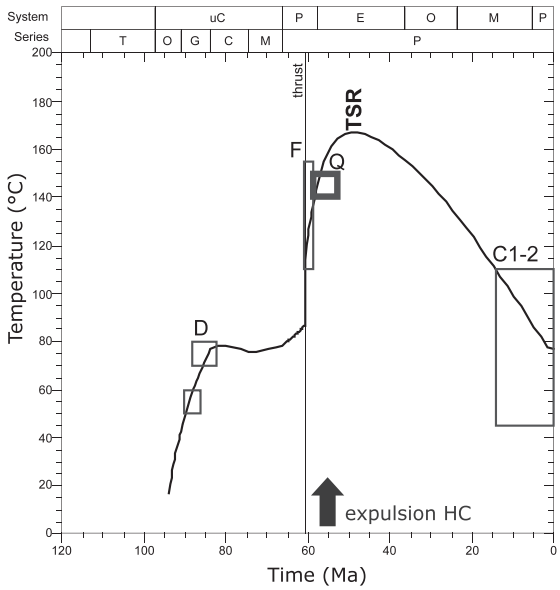

FIG. 4.—Diagenetic data used to calibrate the burial history of the Orizaba Formation in the Córdoba area. The burial curve was modeled by the Genex-1D code (IFP) making use of a kinematic reconstruction in line with inferred eroded thicknesses based on paleopressure calculations. CL = cathodoluminescence; FI = fluid inclusions; HC = hydrocarbons; for location of samples, see Figure 7 (see Ferket et al. [2010] for details).

Cement phase	Petrography	Stable isotopes (‰PDB)	FI	Interpretation
Calcite C3	Common cement phase in breccia-veins that postdate burial stylolites and precede tectonic stylolites CL: non/dull luminescent	$\delta^{18}O$ -5.0 to -13.0 $\delta^{13}C$ +1.0 to +2.5	Primary FI H_2O-NaCl T_h 40-65°C T_m -0.8 to -1.9°C	Early syn-Laramide
Calcite C4	Veins containing biodegraded oil and yellow fluorescent HC FI postdating tectonic stylolites	$\delta^{18}O$ -6.0 to -8.6 $\delta^{13}C$ -0.9 to +1.6	Primary-pseudosecondary HC (no water!) T_h 55.5-89°C 10-17mol% CH4 C9-C12 alkane equivalent	Syn- or early post-Laramide

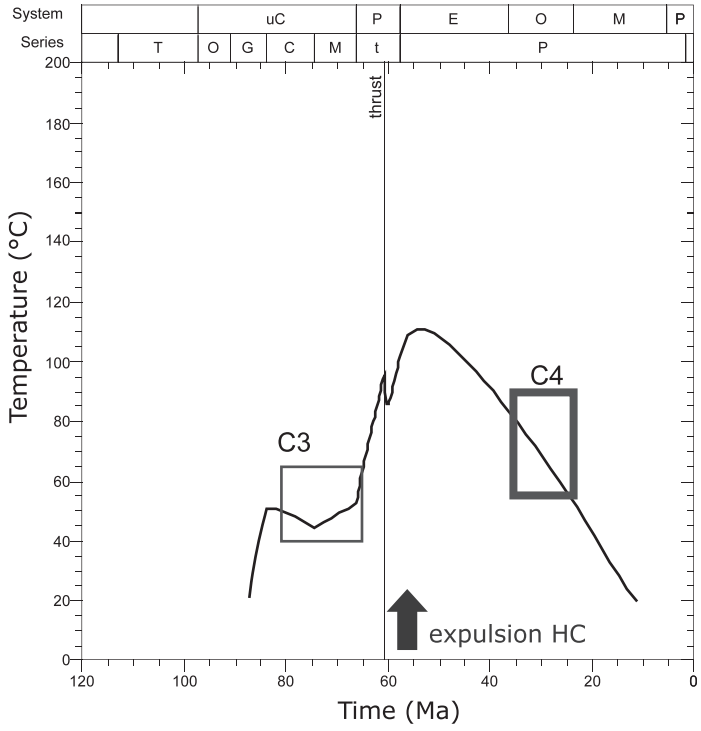

FIG. 5.—Diagenetic data used to calibrate the burial history of the Guzmantla Formation at the Peñuela paleoseep. The burial curve was modeled by the Genex-1D code (IFP) making use of a kinematic reconstruction in line with inferred eroded thicknesses based on paleopressure calculations. CL = cathodoluminescence; FI = fluid inclusions; HC = hydrocarbons; for location of samples, see Figure 7 (see Ferket et al. [2010] for details).

The thickness of the Cretaceous deposits decreases basinward. At this stage, the carbonated sequence displays an eastward dip controlled by the thermal subsidence of the Gulf of Mexico (Fig. 8b).

Santonian–Campanian

During the Santonian, stable platform conditions prevailed, characterized by a subhorizontal configuration and continuous deposition. Under the influence of tectonic load in the internal zones of the Cordillera (Zongolica fold and thrust belt), a flexure of the lithosphere developed in the foreland. These conditions led to local emergence and karstification of the platform in a forebulge domain (Ferket et al. 2000), leading to minor erosion and to the formation of a foredeep (Fig. 8c). In this foredeep, at least 4.5 km of argillaceous carbonated sediments (if not partly related to tectonic stacking) were deposited. It is assumed that the basement had developed a westward tilt by that time (Fig. 8c).

Maastrichtian

This period marks the beginning of the Laramide Orogeny. The first argillaceous carbonates filling the flexural basin(s) were deposited during the Maastrichtian. These sediments probably were particularly well expressed in the foredeep in the western part of the section and thinned to the east (Fig. 8d).

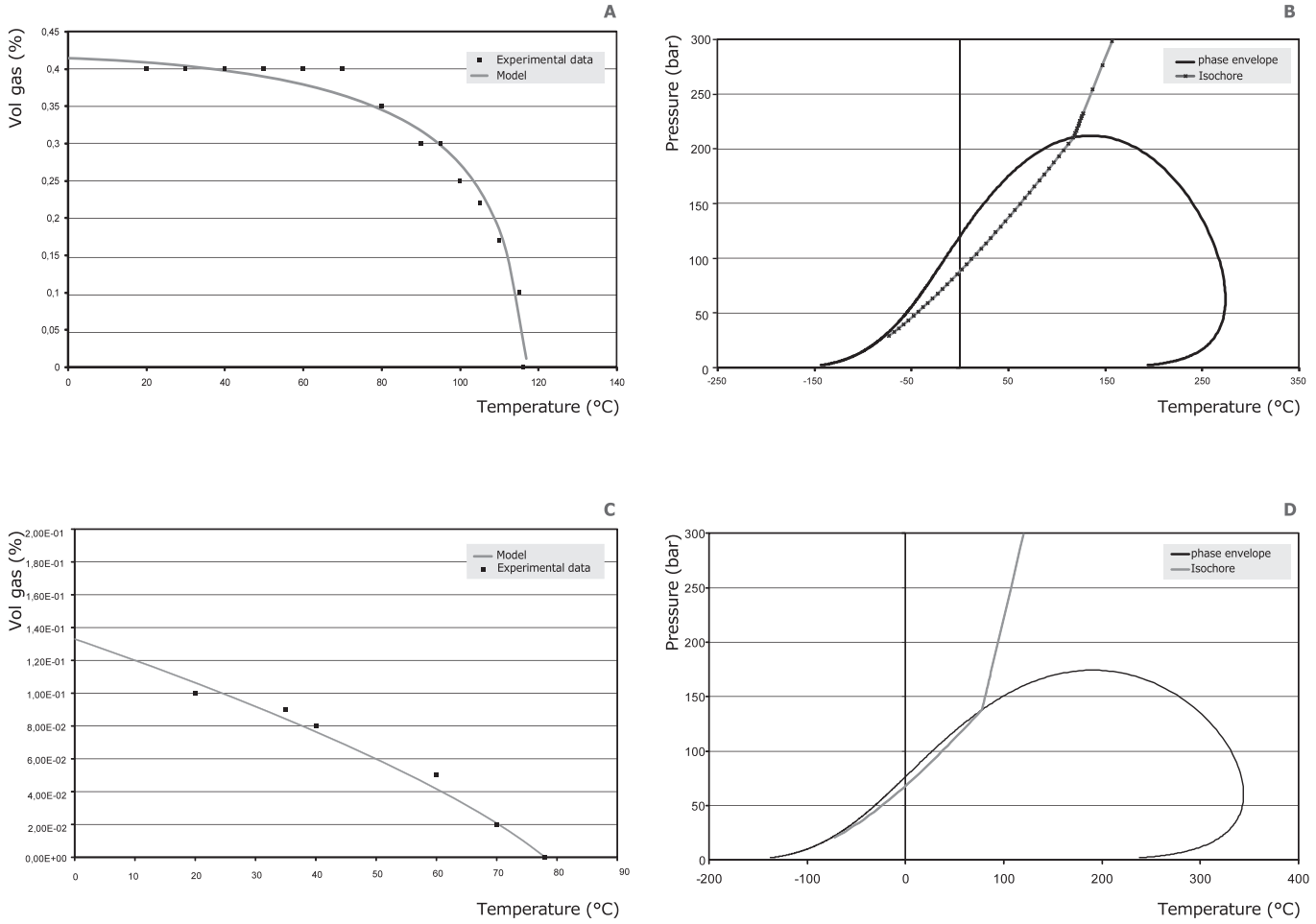

FIG. 6.—Pressure-Volume-Temperature (PVT) modeling for fluid inclusions found in the Córdoba area, respectively, in quartz from a well close to Córdoba (A and B) and in calcite from the Peñuela paleoseep (C and D). The progressive shrinking of the vapor bubble (% volume of gas) of two-phase hydrocarbon inclusions (A and C) is used, together with results from SFTIR analyses, to calculate the liquid-vapor curves of the fluid system entrapped and isochors relative to Th measured (B and D), from which pressure and temperature of the fluid inclusion entrapment were calculated (see Ferket et al. [2010] for details).

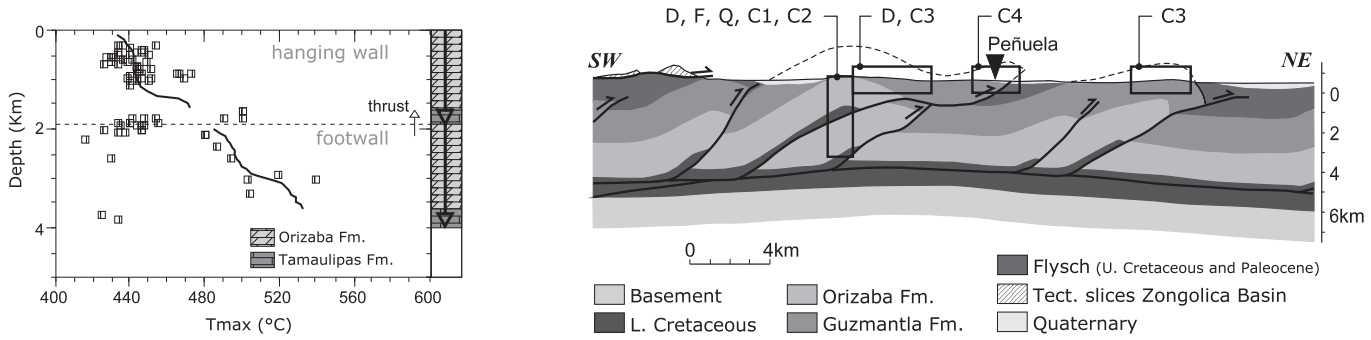

FIG. 7.—Maturity data (T_{max}, squares) used to calibrate thermal modeling (continuous line) in the Córdoba area. The IFP GenTect 1D basin modeling tool is used to model the temperature–depth curve (see detail in Ferket et al. [2010]). The represented model corresponds to a kinematic scenario taking into account an eroded sequence of 4.5 km, as derived from fluid inclusion data and Pressure-Volume-Temperature (PVT) modeling. The present model fits the maturity data much better than do classical concepts that consider higher heat flow and lesser erosion. The cross section gives the location of samples used for diagenetic studies. The letter codes refer to specific minerals that were identified and in which useful fluid inclusions were found (D = dolomite; Q = quartz; C = calcite; F = fluorite).

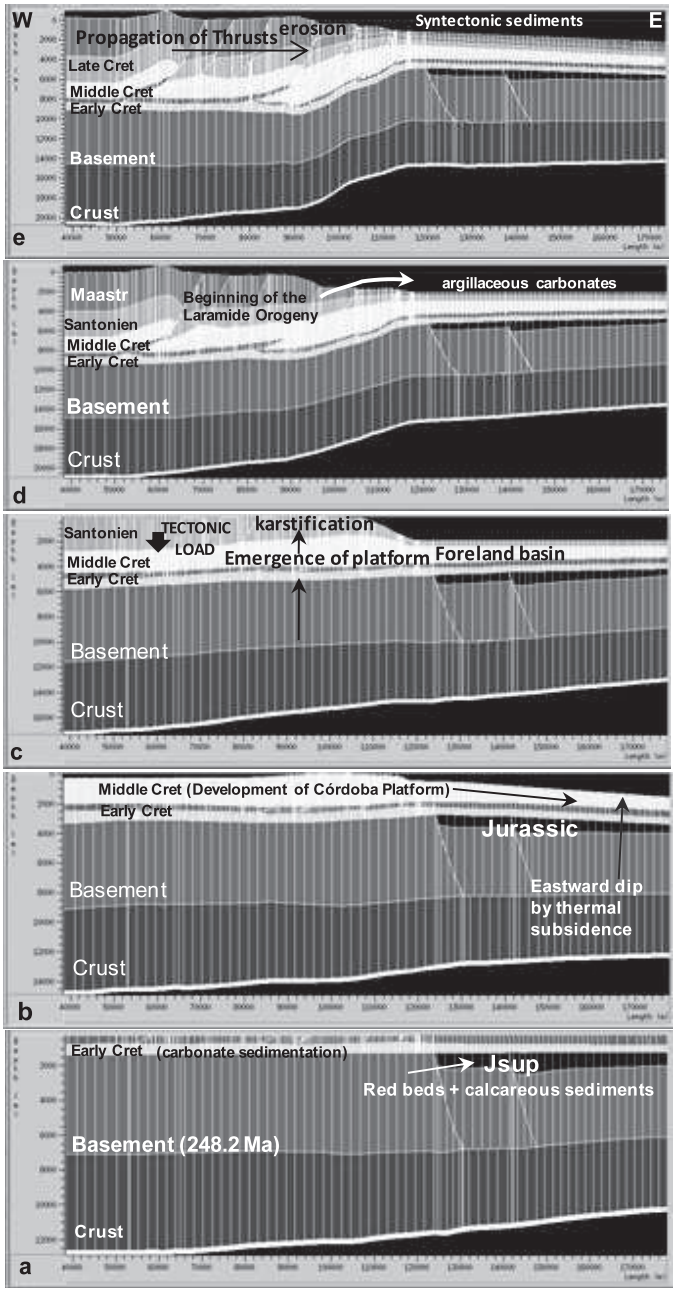

FIG. 8.—Main kinematic steps of section AA', obtained from back-stripping restoration of all lithostratigraphic units. (a–e) Early to Late Cretaceous stages; (f–k) Paleocene to present day.

Paleocene

The Laramide Orogeny continued in the western part of the study area, represented by eastward propagation of thrusts and overthrusting of the Orizaba Platform and Zongolica Basin domains upon the Córdoba Platform. This period is marked by deposition of syntectonic sediments in structural lows and in the Veracruz Basin (Fig. 8e). This period is also characterized by a change in sedimentation in the region, from calcareous sediments to more siliciclastic deposits.

Late Paleocene–Early Eocene

This period is characterized by differences in the thickness of sediments deposited in the folded western border of the Veracruz Basin, recording the onset of Laramide deformation in this zone. Thick accumulation of Lower Eocene sediments in the western part of the basin indicates that the principal phase of deformation in this zone occurred at that time. From this time onward, subsidence caused the basement below the Veracruz Basin to tilt eastward again (Fig. 8f).

Middle Eocene–Late Eocene

Local emergence of the presently buried thrust front occurred during the Late Eocene to Early Oligocene (Ferket 2004, 2006). The last thrust deformation in this zone probably took place around the Middle Eocene. A major change in sedimentation was initiated in the Veracruz Basin starting in the Late Eocene, when the eastern part of the basin subsided faster than the western portion, resulting in an increased eastward tilt of the basement and thicker sedimentary sequences to the east (Fig. 8g).

Oligocene

The Oligocene is characterized by eastward thickening of the sedimentary sequence and continued eastward tilting of the basement below the Veracruz Basin. The Chattian unconformity clearly imaged in seismic lines resulted from a major sea-level drop that marks the end of Oligocene deposition (hiatus) in the basin. The Mata Espino antiformal structure is also interpreted to have initiated during the Oligocene (Fig. 8h).

Early Miocene–Middle Miocene

The Early Miocene is characterized by isopachous strata throughout the Veracruz Basin, indicating that tilting of the basement had decreased by that time. Small variations in sedimentary thickness can be attributed to early transpressional deformation of the basin. By the end of the Middle Miocene, sediments are folded and locally faulted, giving rise to the NVC and Mata Espino structures presented on the modeled section (Fig. 8i).

Upper Miocene

The Upper Miocene series onlaps the antiformal structures and almost fills the basin with strata that thicken to the east. The original westward extent of Miocene sediments over the thrust belt structures is unclear (Fig. 8j).

Pliocene–Recent

Late Miocene to Pliocene reactivation and uplift of frontal structures (possibly in response to basement faults reactivated by transpression) led to uplift of the Laramide Front with erosion of part of the Upper Miocene strata and dragging and steepening of Lower to Middle Miocene strata. A Pliocene piggyback basin formed to the west of the buried tectonic front zone. The Veracruz Basin was filled up further with sediments that started to develop prograding clinoforms (Fig. 8k).

A total tectonic shortening of 25 to 45% was proposed by Amoco–Pemex–IMP (1995) for the Córdoba thrust belt for the Laramide event. Post-Laramide uplift and erosion account for more than 4.5 km of erosion in the Córdoba foothills, as well as farther north in the Sierra Madre Oriental (Gray et al. 2001; Alzaga-Ruiz et al. 2008a, 2008b). Post-Laramide basement uplift is also associated with extensional structures in the hinterland and strong erosion in the foothills farther

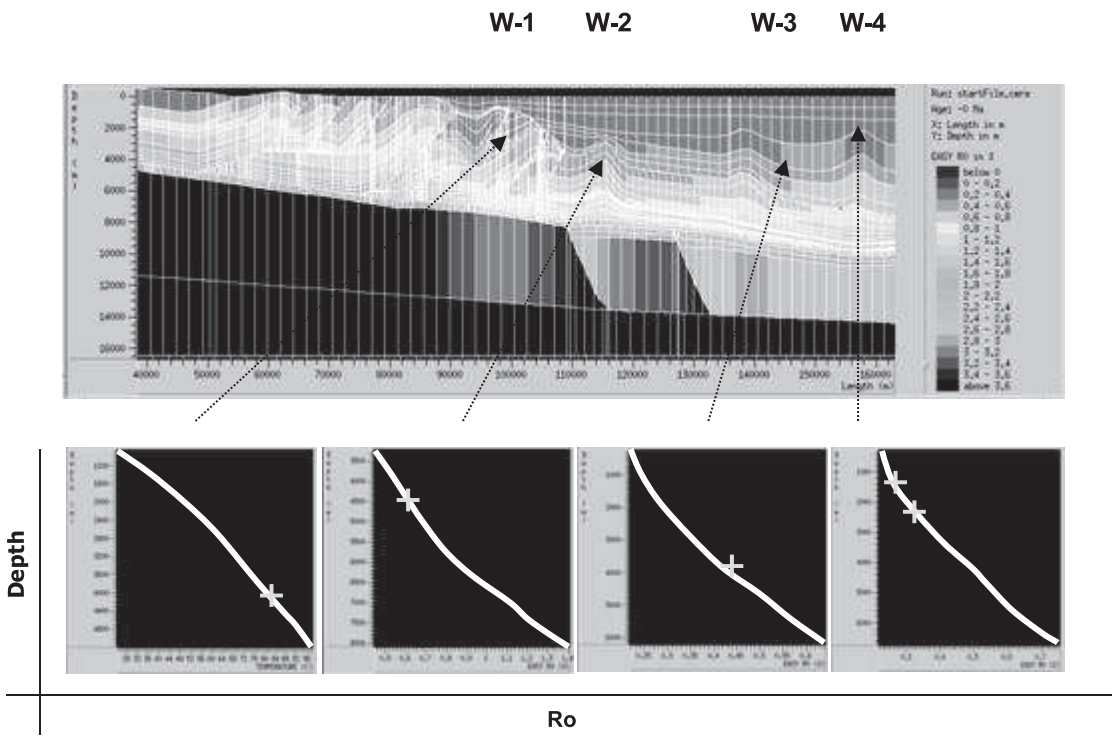

FIG. 9.—Thermal calibration of the Ceres model by means of R_o (location of the wells used for calibration is indicated by labels W1 to W4, indicated by small white symbols).

north in the Cordillera, similar to the Basin and Range province in the United States and to the Canadian Rockies (Hardebol et al. 2007, 2009; Roure et al. 2010). Unlike other thrust belts, however, the basement below the foothills is currently tilted toward the foreland. These uplift and unroofing processes can be explained by post-Laramide asthenospheric upwelling beneath the entire length of the North American Cordillera, a Pacific subduction-related "corner flow" thinning the continental crust and forcing uplift of the Córdoba thrust belt relative to the more stable Veracruz area, which continued to subside (Hyndman et al. 2005; Alzaga-Ruiz et al. 2008a, 2008b; Roure 2008; Roure et al. 2010).

THERMAL CALIBRATION AND RESULTS OF THE THERMAL MODELING

Thermal Calibration

Calibration of the thermal model was based on well data along the modeled section, including BHT, geothermal gradient, and core porosity data from wells located in Veracruz Basin and from T_{max} and R_o (vitrinite reflectance in oil) trends. Multiple simulations of 1D well models were initially carried out to constrain the thermal model. Additional temperature data from fluid inclusion studies was used to run a new set of 1D thermal models with the aim of constraining past heat flow values, which fit both the present-day temperature and maturity data and the FI burial (Ferket 2006, Ferket et al. 2010). The result of this calibration is a basal heat flow history starting with values of up to 50 mW/m^2 for the pre-Laramide periods and decreasing to 30 mW/m^2 for the post-Laramide period (Table 2). Several simulations employing both hydrostatic and nonhydrostatic conditions were carried out making use of these heat flow values for the calibration of the 2D basin models. A satisfactory agreement between well data and calibration was obtained from CERES2D simulations (Fig. 9).

Thermal Maturity Evolution

Lower and Middle Cretaceous source rocks located in the Córdoba Platform entered the oil window as early as 80 My, whereas the gas window was reached at 62 My (Fig. 10). This early maturation resulted from the early deep burial in this area. In contrast, Upper Jurassic source rocks in the Veracruz Basin entered the oil window at 45 My and the gas window at 39 My (Fig. 10). The increase of heat flow boundary conditions to ensure a reasonable fit with the temperature and vitrinite data led to an earlier generation of oil than was forecasted by the Genex modeling (see Fig. 4), but the timing of expulsion of the hydrocarbon from the source rocks is unchanged, as it depends on the expulsion saturation threshold, which is still reached during the Early Tertiary. Thus, the coupling between deformation and migration is still properly modeled.

Lower and Middle Cretaceous source rocks of the Veracruz Basin reached the oil window from 42 My onward, whereas the gas window was reached at 24 My. For the Paleocene source rocks in the basin, the CERES2D calculations indicate that they entered the oil and gas windows at 29 My and 1 My, respectively (Fig. 10). Upper Paleocene and Lower Eocene source rocks entered the oil window from 15 My onward (Fig. 10), whereas Middle Eocene and Upper Eocene source rocks entered the oil and gas windows at 11 My and 9 My, respectively (Figs. 10, 11). Tertiary source rocks have not yet reached the gas window as a result of lack of sufficient burial (Figs. 10, 11), although they may have produced biogenic gas. Finally, the potential Oligocene source rock is presently immature, except in the east (Fig. 10), where source rocks entered the oil window at 3 My (Figs. 10, 11).

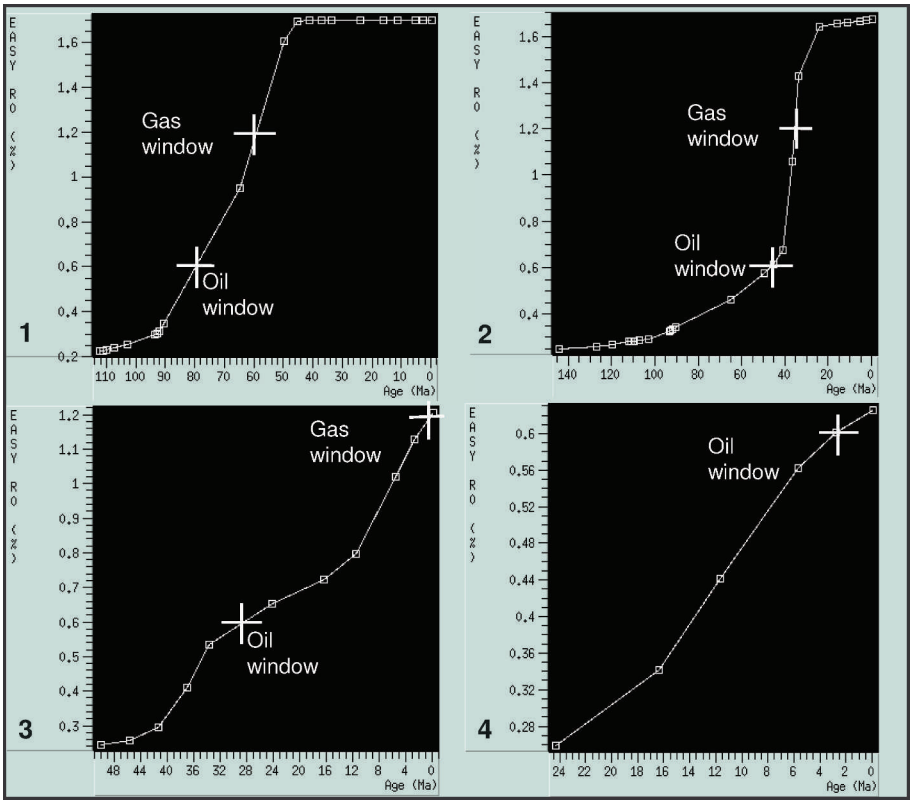

FIG. 10.—Diagrams showing the time at which different source rocks entered the oil and gas windows in the Córdoba Platform and Veracruz Basin: (1) Cretaceous source rocks from the Córdoba Platform; (2) Jurassic source rocks; (3) Lower Paleocene source rocks; (4) Oligocene source rocks from the Veracruz Basin. Large plus symbols indicate the time at which the source rock entered the oil or gas window.

Transformation Ratio

The "transformation ratio" (TR) parameter indicates the evolution stage of the kerogen, specifically addressing what proportion of the hydrocarbons has been produced with respect to the maximum potential hydrocarbon yield. These calculations are based on the kinetic parameters of Behar et al. (1997). Upper Jurassic and Lower to Middle Cretaceous source rocks located in the deepest parts of the Veracruz Basin have TR values measuring higher than 85%, indicating that these intervals have generated nearly all the possible hydrocarbons. Lower and Middle Cretaceous source rocks, located at the former platform-to-basin transition, also appear to have produced hydrocar-

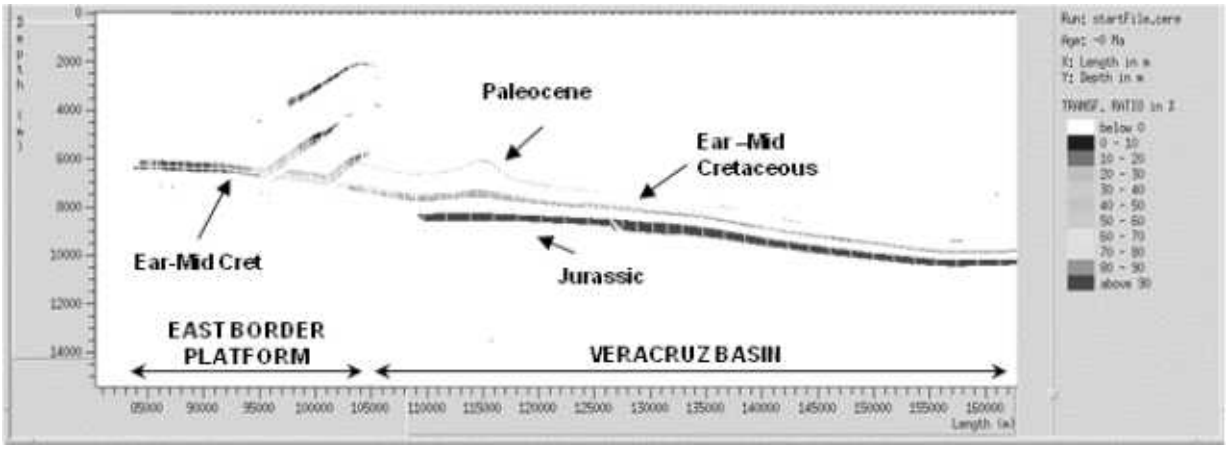

FIG. 11.—Present-day distribution of transformation ratio (ratio between the source rock potential and the effectively produced hydrocarbons) for different source rocks, according to their location.

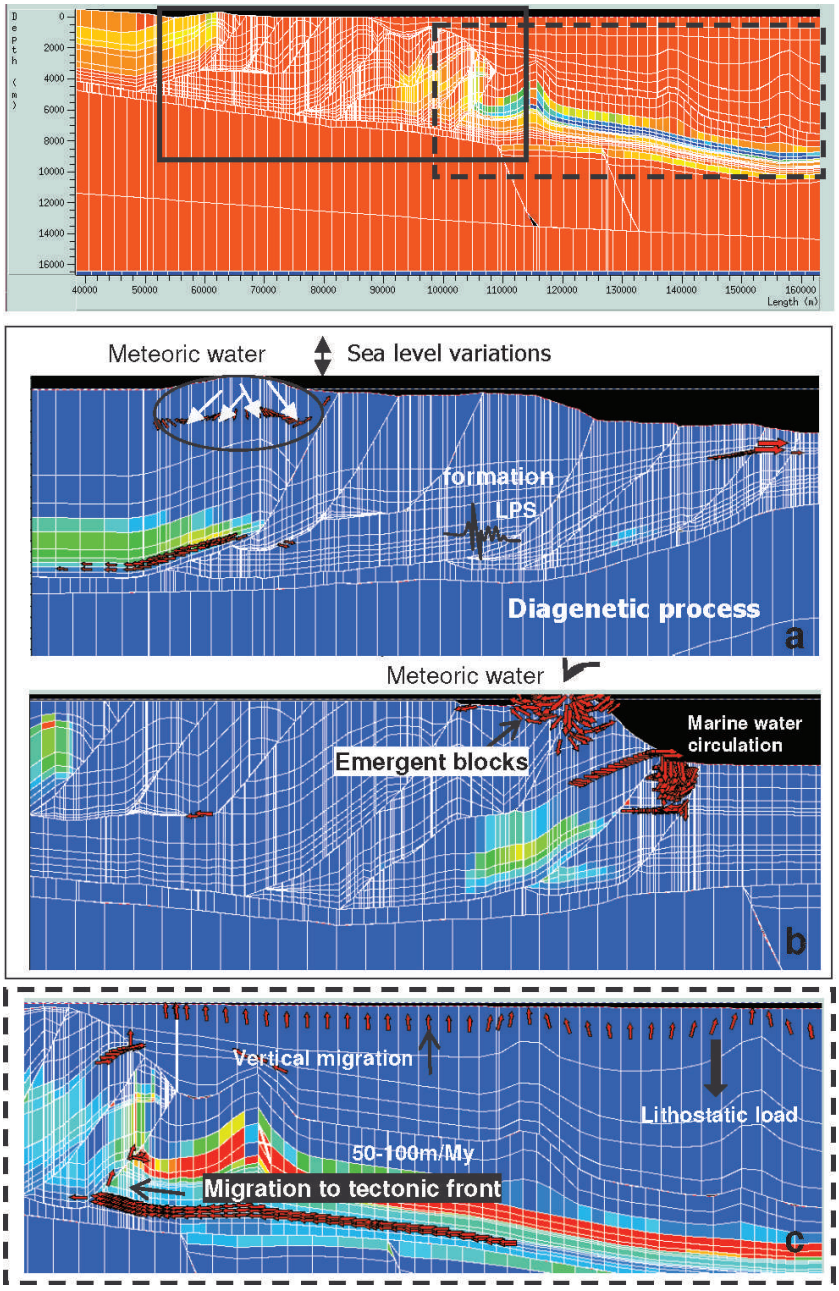

FIG. 12.—Top: Present-day architecture of the thrust front, with a rectangle localizing the two bottom inserts. Bottom: fluid flow simulations: (a) past architecture of this part of the section during the Campanian showing three flow systems: meteoric influx due to karstification of the emerged forebulge, squeegee flow toward the east and westward flow in isolated thrust compartments; (b) Early Eocene stage, showing (1) meteoric influx in locally emerged structures at the tectonic front, (2) westward flow toward the tectonic front from shale dewatering in the basin, and (3) eastward squeegee flow from the front toward the basin; (c) Late Miocene stage showing flow in the Veracruz Basin. Vertical fluid escape due to increased lithostatic load is the predominant mechanism with a continuous escape of basinal fluids. If a Cretaceous source rock is assumed, the model also predicts the onset of hydrocarbon migration from the basin up-dip to the tectonic front, with velocities ranging from 50 to 100 m/My.

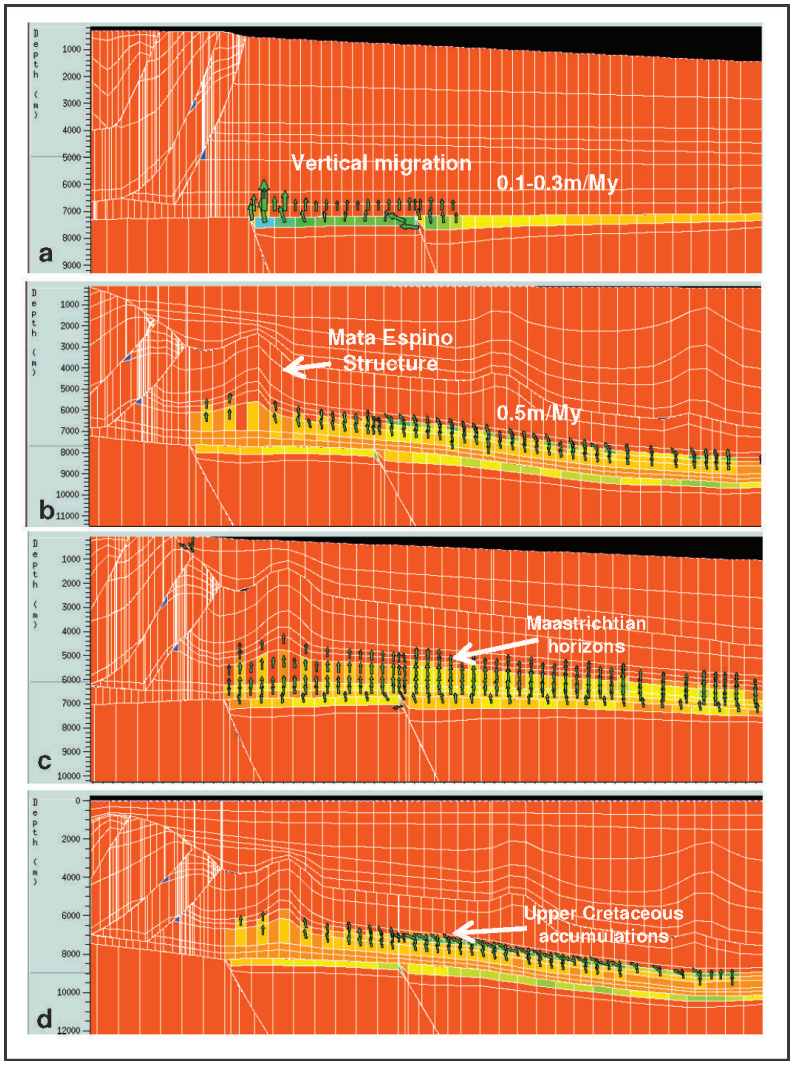

FIG. 13.—Hydrocarbon migration simulated for a Jurassic source rock located in the Veracruz Basin. (a) Late Eocene situation, (b) Early Miocene, (c) Late Miocene, (d) present day (see text for explanation).

bons. Similar source rocks located at the eastern border of the Córdoba Platform are characterized by average TR values below 60%, which implies that they may still be actively producing late oil or gas condensate. Such low maturity is a result of early uplift of the Laramide thrust belt (Fig. 11).

FLUID FLOW RECONSTRUCTION AND HISTORY OF HYDROCARBON MIGRATION

Scenario of Ancient Fluid Circulations and Comparison with the Data

The calculations carried out by CERES2D show a history of fluid migration, starting from the Maastrichtian in the western part of the section (Fig. 12a). Concurrently with the eastward propagation of the thrust belt, expulsion of fluids took place in the then-undeformed parts of the foreland, which recorded an early episode of layer parallel shortening (cf. Ferket et al. 2004). Formation fluids migrated up-dip along the foreland flexure, in the eastern part of the section (squeegee flow; Oliver 1986, Machel and Cavell 1999). Tectonic and burial compaction led to overpressures and expulsion of fluids, resulting in hydrofracturing and brecciation followed by precipitation of minerals with a different diagenetic signature (from stable isotope data) than is associated with the host rock (Ferket et al. 2003, 2004, 2006, 2010; Ferket 2004, 2006).

Ultimately, folding of the strata created additional fracture porosity (Fig. 12b). Locally, porosity was further enhanced by fluid circulations related to thermochemical sulfate reduction (in the deeply buried anhydrite-bearing intervals) or to karst development (in emerged structures). In contrast to the early eastward-directed squeegee flow, fluid flow in the already-compartmentalized thrust blocks in the western part of the section occurred from east to west, from the high-pressured zone of the ramp folds to their passive limbs. Such flow was focused at the base of the Middle Cretaceous dolomites and reached a mean velocity of 10 m/My.

During the Middle Eocene, the tectonic front had reached the eastern platform border and locally emerged in this easternmost zone. Meteoric water could thus enter the reservoirs and cause karstification below the presently buried Laramide unconformity (Fig. 12b). Simultaneously,

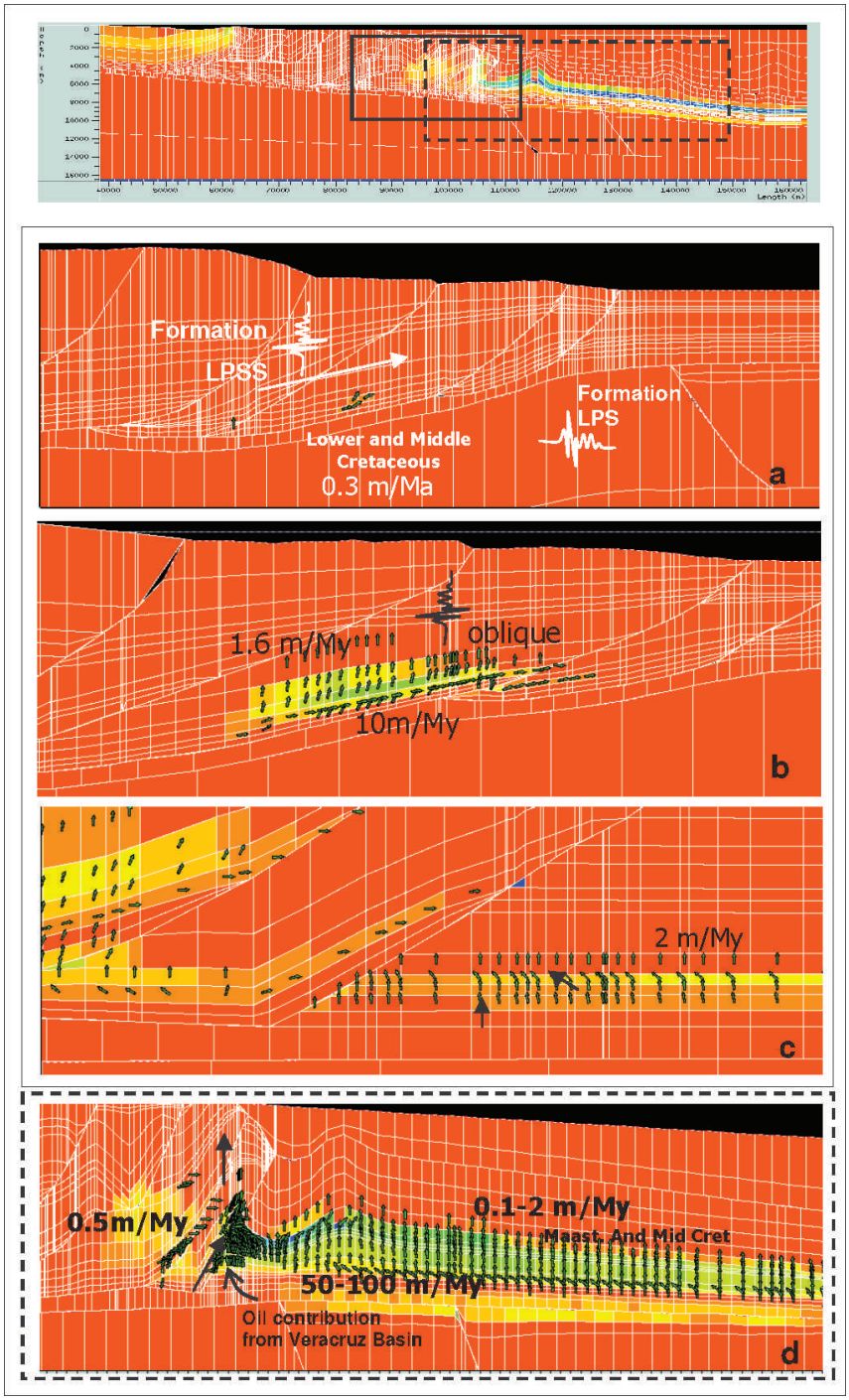

FIG. 14.—Hydrocarbon migration simulated for a model with two source rock horizons, in the Jurassic and Cretaceous series, respectively. Top: Present-day architecture of the thrust front, with a rectangle localizing the bottom inserts; Bottom: (a) Paleocene stage, (b) Early Eocene, (c) Late Eocene, (d) Early to Middle Miocene (see text for explanation). LPS = layer parallel shortening and associated stylolites; CS = compaction-related stylolites.

marine water circulation also took place in two directions, between the Córdoba Platform and the Veracruz Basin, associated with shale dewatering and continued squeegee flow (Fig. 12b).

During and following the Late Eocene, vertical fluid escape due to the increased lithostatic load became predominant in the Veracruz Basin (Fig. 12c). If a Cretaceous source rock is assumed, the model also predicts the onset of hydrocarbon migration from the basin up-dip to the tectonic front, with velocities ranging from 50 to 100 m/My (see

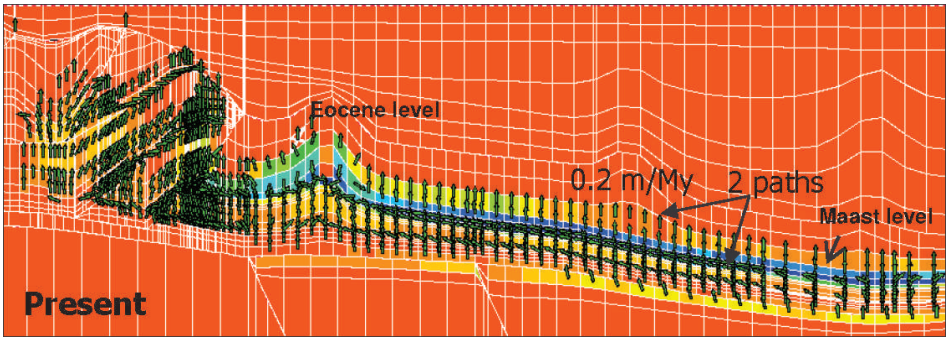

FIG. 15.—Hydrocarbon migration at present time. Note that oil has reached the Eocene reservoirs in the Veracruz Basin, with a velocity decrease down to 0.2 m/My.

below). This migration accelerated (~100 m/My) by the Late Miocene and was directed toward the tectonic front and upward along faults. Presently, the westward migration up to the tectonic front at the base of the Middle Cretaceous still represents the dominant flow pattern. Migration velocities of approximately 60 m/My are presently associated with vertical dewatering of the Tertiary series (Fig. 12c).

Hydrocarbon Migration History

As mentioned above, the Cretaceous platform carbonates in the easternmost frontal thrust zone produce oil and gas, whereas Tertiary clastic rocks in the Veracruz Basin produce only gas. As a result of current numerical limitations of CERES2D, migration paths could only be calculated for two-phase fluid flow (i.e., water and oil), thus excluding natural gas. The distribution and role of different source rocks in the eastern tectonic front and westernmost Veracruz Basin area are controversial, because the oils lack a typical Jurassic signature, and the existence of Cretaceous intraplatform source rocks is still questioned (Ferket 2004, 2006; Vázquez 2004). In order to respond to these uncertainties, two models have been constructed, and various simulations were run to test the impact of source rock distribution and other source rock characteristics. The first model considered only Upper Jurassic source rocks present in the Veracruz Basin. The second model assumes both Jurassic source rocks in the Veracruz Basin and Cretaceous source rocks located within the Veracruz Basin and in the eastern part of the platform. The model output defines water saturations, which are complimentary to hydrocarbon (in this case oil) saturation.

In the first model, which considers only Jurassic source rocks, oil migration starts during the Late Eocene (~37 Ma) in the westernmost part of the basin. Migration takes place vertically and the velocity is low (0.1–0.3 m/My; Fig. 13a). By the Early Miocene (~16 My) the velocity increased to 0.5 m/My and the migration front moved up to the Upper Cretaceous strata, filling the Mata Espino structure (Fig. 13b). A very minor westward migration toward the tectonic front occurred at this time. During the Late Miocene, the migration front has reached the Maastrichtian horizons (Fig. 13c), and velocity remained constant at ~0.5 m/My. At present, the hydrocarbon migration from Jurassic source rocks is vertical, and there is no significant migration toward the tectonic front. Therefore, traps are situated mainly in the Upper Cretaceous of the Veracruz Basin (Fig. 13d).

In the second model, hydrocarbon migration started at 65 My for source rocks located in the eastern part of the platform. Flow was concentrated at the Lower to Middle Cretaceous level and directed to the east with a velocity of 0.3 m/My (Fig. 14a). By the Early Eocene (~50 My; Fig. 14b) a complex migration pattern prevailed in the thrust belt. An eastward-directed migration of 10 m/My occurred at the Lower to Middle Cretaceous level following faults, whereas shallower levels exhibited vertical migration of hydrocarbons with a slower velocity of about 1.6 m/My (Fig. 14b). The same pattern continued during the Late Eocene (~37 My), but at this time hydrocarbon migration also started in the Veracruz Basin, with vertical and westward-directed flow of less than 2 m/Ma (Fig. 14c). By the Oligocene (~34 My), the oil migrated further upward along faults in the tectonic front, and a larger contribution (~5 m/My) from the Veracruz Basin helped charge the reservoirs in this zone. The oil migration front reached the Santonian level in the tectonic front by that time. At the beginning of the Miocene (~24 My), hydrocarbon migration became more rapid, with velocities around 50 m/My, and was directed both eastward along faults located in the eastern part of the platform and vertically in the Veracruz Basin. The velocities of upward migration in the Veracruz Basin were low (0.1–2 m/My). The Middle Miocene (~16 My; Fig. 14d) was characterized by slower eastward and upward migration (0.5 m/My). Nevertheless, westward migration from source rocks in the Veracruz Basin toward and through the tectonic front continued to contribute to the oil charge. This flow was concentrated mainly at the Maastrichtian and Middle Cretaceous levels (Fig. 14d). Presently (0 My; Fig. 15), the flow patterns in the Córdoba Platform remain the same, whereas the Veracruz Basin is characterized by a complex migration pattern. Below the Maastrichtian level flow is directed to the tectonic front in the west. Above this level a vertical migration predominates, with low velocities around 0.2 m/My. The model predicts that the oil migration currently has reached the Eocene level (Fig. 15).

CONCLUSIONS

Fluid inclusion data in the Córdoba Platform are consistent with the occurrence of a former Late Cretaceous–Paleocene flexural sequence that was up to 4.5 km thick, prior to uplift and removal by erosion. Accordingly, the present east-dipping attitude of the basement is best interpreted as the result of post-Laramide upwelling of the mantle beneath the North American Cordillera. This change in the dipping attitude of the basement was coeval with a rapid transfer of siliciclastic erosional products from the thrust belt toward the Veracruz Basin. This resulted in an increase in the source rock burial, which then entered the oil window in the basin.

The 2D fluid flow simulations presented here considered both Jurassic and Cretaceous series from the Veracruz Basin as potential source rocks. Flow simulation results are consistent with the known petroleum occurrences in this region. The source rocks located in the platform entered the oil window at 80 My, whereas the source rocks in the basin entered the oil window at 45 My. The first pulses of migration started at roughly the end of the Late Cretaceous (65 My). Migration

paths changed through time. Initially migration was dominantly vertical, with rates that increased gradually from 0.3 to 2 m/My. With the increase in the lithostatic load in the basin and the corresponding increase in pore pressure, fluids started to migrate toward the tectonic front, which had already been deformed and contained potential structural traps when hydrocarbon migration started. During the Eocene and the Oligocene, hydrocarbons migrated with a mean velocity of 50 m/My (with velocities potentially reaching as high as 100 m/My from the basin toward the folded chain, as a result of the progressive inversion of the tilting). The speed of migration decreased to 0.5 m/My during the Lower Miocene.

As a result of numerical limitations, the present model could only simulate the fluid flow of both water and oil but not of gas. Nevertheless, it shows that oil could not reach stratigraphic levels shallower than the Eocene within the Veracruz Basin itself. This finding is consistent with the observations that in the Veracruz Basin, the Miocene series only host gas reservoirs, and the few oil wells in the basin produce from Eocene reservoirs. The fluid flow modeling is consistent with the various stages of water displacement recorded in the various stages of cementation.

ACKNOWLEDGMENTS

IMP provided the logistics for the fieldwork, and Pemex provided access to subsurface data. The authors acknowledge the work done by the CERES2D development and maintenance teams during many years: Isabelle Faille, Catherine Marquer (IFP New Energies), and Hervé Devoitine (Tech-Advantage). We are grateful to Pascal Mougin for the thermodynamic modeling and to Biliana Gasharova and Y.L. Mathis at the Institute for Synchrotron Radiation (ANKA beamline; Karlsruhe) for helpful assistance at the FTIR beam line. We thank E. Hiemstra and Editor N. Harris for the thorough reviews and improvement of the manuscript.

REFERENCES

Alzaga-Ruiz H, Granjeon D, Lopez M, Séranne M, Roure F. 2008a. Gravitational collapse and Neogene sediment transfer across the western margin of the Gulf of Mexico: Insights from numerical models. *Tectonophysics* doi:10.1016/j.tecto.2008.06.017.

Alzaga-Ruiz H, Lopez M, Roure F, Séranne M. 2008b. Interactions between the Laramide foreland and the passive margin of the Gulf of Mexico: Tectonics and sedimentation in the Golden Lane area, Veracruz State, Mexico. *Marine and Petroleum Geology* doi:10.1016/j.marpetgeo.2008.03.009.

Amoco–Pemex–IMP. 1995. Tertiary stratigraphy, basin evolution and economic potential of the Veracruz Basin, East–Central Mexico. Pemex Internal Report, 78 p.

Behar F, Espitalie J, Marquis F, Tang Y, Vandenbroucke M. 1997. Thermal cracking of kerogen in open and closed systems: Determination of kinetic parameters and stochiometric coefficients for oil and gas generation. *Organic Geochemistry* 26:321–339.

Berman AE, Pérez-Cruz G, Cantu-Chapa C. 1995. Tertiary stratigraphy, basin evolution and economic potential of the Veracruz Basin, East-Central Mexico. Pemex Internal Report, 78 p.

Bessis F, Burrus J, Chenet PY, Doligez B, Ungerer P. 1990. Basin evaluation by integrated two-dimensional modelling of heat transfer, fluid flow, hydrocarbon generation and migration. *American Association of Petroleum Geologists Bulletin* 74:309–335.

Campa MF, Coney PJ. 1983. Tectonostratigraphic terrane and mineral resources distribution in Mexico. *Canadian Journal of Earth Sciences* 13:1040–1051.

Chenet PY, Doligez B, Schmerber G. 1986. The Themis model: A new tool for the hydrocarbon exploration: Integrated study of the sedimentary basin from the sedimentation to the hydrocarbon accumulation. *Hidrocarburos, 1° Congreso Latino–Americano*, Buenos Aires, May 4–11 1986. 10:5187–5202.

Divies R, Sassi W. 1996. Foldis: Forward modelling of folding and compaction. *Annales Geophysicae* 14:1, C106.

Doligez B (Editor). 1987. *Migration of Hydrocarbons in Sedimentary Basins*: Editions Technip, Paris. 712 p.

Espinoza NM, Toriz GJ. 2005. Structural styles in the Veracruz area. *Review of the Mexican Association of Exploration Geophysicists* 4:3–20 (in Spanish).

Faille I, Nataf F, Schneider F, Willien F. 1998. Domain decomposition methods for fluid flows in porous medium. *In* Proceedings of the ECMOR 6th European Conference on the Mathematics of Oil Recovery; September 8–11, 1998; Peebles. Paper B-06, 6 p.

Ferket H. 2004. Sedimentology, diagenesis and fluid flow reconstruction in the Laramide fold-and-thrust belt of eastern Mexico (Córdoba Platform): Implications for petroleum exploration [PhD doctoral thesis]: Katholieke Universiteit Leuven, 281 p.

Ferket H. 2006. Kinematic evolution, diagenesis and fluid flow reconstruction in the Laramide fold-and-thrust belt of eastern Mexico (Córdoba Platform and Veracruz Basin): Implications for petroleum exploration. Institut Français du Pétrole Report, 123 p.

Ferket H, Guilhaumou N, Roure F, Swennen R. 2010. Insights from fluid inclusions, thermal and PVT modelling for paleoburial and thermal reconstruction of the Córdoba petroleum system (NE Mexico). *Marine and Petroleum Geology* 28:936–958.

Ferket H, Ortuño S, Swennen R, Roure F. 2003. Diagenesis and fluid flow history in reservoir carbonates of the Cordilleran fold- and thrust- belt: The Córdoba Platform. *In* Bartolini C, Burke K, Buffler R, Blickwede J, Burkart B (Editors). *Mexico and the Caribbean Region: Plate Tectonics, Basin Formation and Hydrocarbon Habitats*, Memoir 79: American Association of Petroleum Geologists, Tulsa, Oklahoma. p. 283–304.

Ferket H, Roure F, Swennen R, Ortuño S. 2000. Fluid migration placed into the deformation history of fold-and-thrust belts: An example from the Veracruz Basin (Mexico). *Journal of Geochemical Exploration* 69–70:275–279.

Ferket H, Swennen R, Ortuño-Arzate S, Cacas MC, Roure F. 2004. Hydrofracturing in the Laramide foreland fold-and-thrust belt of Eastern Mexico. *In* Swennen R, Roure F, Granath J (Editors). *Deformation, Fluid Flow and Reservoir Appraisal in Foreland Fold-and-Thrust Belts*, Hedberg Series, Memoir 1: American Association of Petroleum Geologists, Tulsa, Oklahoma. p. 133–156.

Ferket H, Swennen R, Ortuño-Arzate S, Roure F. 2006. Fluid flow evolution in petroleum reservoirs with a complex diagenetic history: An example from Veracruz, Mexico. *Journal of Geochemical Exploration* 89:108–111.

Gonzalez-Mercado GE. 2007. Reconstruction des circulations de fluides et de la migration des hydrocarbures (modélisation Ceres 2D) le long d'un transect à travers la Plateforme de Córdoba et le Bassin de Véracruz, Mexique. DES Université Pierre et Marie Curie. Institut Français du Pétrole Report 60112, 40 p.

Gray GG, Pottorf RJ, Yurewicz DA, Mahon KI, Pevear DR, Chuchla RJ. 2001. Thermal and chronological record of syn- and post-Laramide burial and exhumation, Sierra Madre Oriental, Mexico. *In* Bartolini C, Buffler RT, Cantu-Chapa A (Editors). *The Western Gulf of Mexico Basin: Tectonics, Sedimentary Basins and Petroleum Systems*, Memoir 75: American Association of Petroleum Geologists, Tulsa, Oklahoma. p. 159–181.

Guilhaumou N, Benchilla L, Mougin P, Dumas P. 2004. Advances in hydrocarbon fluid inclusions microanalysis and PVT modelling: Diagenetic history, P-T and fluid flow reconstruction, a case study in the North Potwar Basin, Pakistan. *In* Swennen R, Roure F, Granath J (Editors). *Deformation, Fluid Flow and Reservoir Appraisal in Foreland Fold-and-Thrust Belts*, Hedberg Series, Memoir 1: American Association of Petroleum Geologists, Tulsa, Oklahoma. p. 5–21.

Guilhaumou N, Dumas P. 2005. Synchrotron FTIR hydrocarbon fluid inclusions microanalysis applied to diagenetic history and fluid flow reconstruction in reservoir appraisal. *Oil and Gas Science Technology Revue de l'Institut Français du Pétrole* 60(5):1–12.

Guzman-Vega ME, Castro OL, Roman RJR, Medrano ML, Valdéz LC, Vàzquez CE, Ziga RG. 2001. Classification and origin of petroleum in the Mexican Gulf Coast Basin: An overview. *In* Bartolini C, Buffler RT, Cantu-Chapa A (Editors). *The Western Gulf of Mexico Basin: Tectonics, Sedimentary Basins and Petroleum Systems*, Memoir 75: American Association of Petroleum Geologists, Tulsa, Oklahoma. p. 127–142.

Hardebol N, Callot JP, Bertotti JL, Faure JL. 2009. Sedimentary and tectonic burial history appraisal and consequent temperature and organic maturation

evolution in thrust-belt systems: A study on the SE Canadian Cordillera. *Tectonics* 28:TC3003, doi:10.1029/2008TC002335.

Hardebol NJ, Callot JP, Faure JL, Bertotti G, Roure F. 2007. Kinematics of the SE Canadian foreland fold and thrust belt: Implications for the thermal and organic maturation history. *In* Lacombe O, Lavé J, Roure F, Vergés J (Editors). *Thrust Belts and Foreland Basins*: New Frontiers in Earth Sciences: Springer-Verlag, Heidelberg, Germany. p. 179–202.

Hyndman RD, Currie CA, Mazzotti SP. 2005. Subduction zone backarcs, mobile belts, and orogenic heat. *Geological Society of America Bulletin* 15(2):4–10.

Jacobo AJ. 1986. The basement of the Poza Rica district and its controls on hydrocarbon generation. Internal review of the Mexican Petroleum Institute 18(1):5–24 (in Spanish).

Jennette DC, Fouad K, Wawrzyniec T, Dunlap D, Muñoz R, Meneses-Rocha J. 2003a. Slope and basin-floor reservoirs from the Miocene and Pliocene of the Veracruz Basin, south-eastern Mexico. *Marine and Petroleum Geology* 20:587–600.

Jennette DC, Wawrzyniec T, Fouad K, Dunlap D, Meneses-Rocha J, Grimaldo F, Muñoz R, Barrera D, Williams-Rojas CT, Escamilla-Herrera A. 2003b. Traps and turbidite reservoir characteristics from a complex and evolving tectonic setting, Veracruz Basin, south-eastern Mexico. *American Association of Petroleum Geologists Bulletin* 87:1599–1622.

Machel HG, Cavell PA. 1999. Low-flux, tectonically-induced squeegee fluid flow ("hot flash") into the Rocky Mountain foreland basin. *Bulletin of Canadian Petroleum Geologists* 47:510–533.

Meneses-Rocha JJ, Rodriguez-Figueroa D, Toriz-Gama J, Banda-Herandez J, Herandez-de La Fuente R, Valdivieso-Ramos V. 1997. *Field Guide to the Geologic Field Trip to the Zongolica Fold-and-Thrust Belt*: Associacion Mexicana de Geologos Petroleros-AMPG.

Ortuño AS. 1991. Contribution de la sédimentologie et de la télédétection à la reconstitution du bassin de Zongolica (Mexique centro-oriental). Place dans la dynamique du couple Golfe du Mexique-Système Cordillérain [PhD thesis]: University of Pau, France, 289 p.

Ortuño AS, Ferket H, Cacas MC, Swennen R, Roure F. 2003. Late Cretaceous carbonate reservoirs in the Córdoba Platform and Veracruz Basin (Eastern Mexico). *In* Bartolini C, Burke K, Buffler R, Blickwede J, Burkart B (Editors). *Mexico and the Caribbean Region: Plate Tectonics, Basin Formation and Hydrocarbon Habitats*, Memoir 79: American Association of Petroleum Geologists, Tulsa, Oklahoma. p. 476–514.

Ortuño AS, Roure F, Cacas MC, Swennen R, Ferket H. 1999. Subtrap Mexican transects across the Córdoba Platform. Institut Français du Pétrole-SUBTRAP (SUBThrust Reservoir APpraisal) Report 45635–2.

Pemex-Schlumberger. 2000. Petroleum map of the Veracruz Basin. Pemex.

Pindell JL. 1994. Evolution of the Gulf of Mexico and the Caribbean. *In* Donovan SK, Jackson TA (Editors). *Caribbean Geology: An Introduction*: University of West-Indies Press, Kingston, Jamaica. p. 13–39.

Prost G, Aranda-Garcia M. 2001. Tectonics and hydrocarbon systems of Veracruz Basin, Mexico. *In* Bartolini C, Buffler RT, Cantu-Chapa A (Editors). *The Western Gulf of Mexico Basin: Tectonics, Sedimentary Basins and Petroleum Systems*, Memoir 75: American Association of Petroleum Geologists, Tulsa, Oklahoma. p. 271–291.

Rojas L. 1999. The tectonic evolution of the Zongolica flood-thrust belt and the Veracruz Basin, eastern Mexico [Master thesis]: Royal Holloway, University of London, 72 p.

Roure F. 2008. Foreland and hinterland basins: What controls their evolution? *Swiss Journal of Earth Sciences* 101(1):5–29. doi:10.1007/s00015–008-1285-x.

Roure F, Andriessen P, Callot JP, Faure JL, Ferket H, Gonzales E, Guilhaumou N, Lacombe O, Malandin J, Sassi W, Schneider F, Swennen R, Vilasi N. 2010. The use of paleo-thermo-barometers and coupled thermal, fluid flow and pore fluid pressure modelling for hydrocarbon and reservoir prediction in fold and thrust belts. *In* Goffey GP, Craig J, Needham T, Scott R (Editors). *Hydrocarbons in Contractional Belts*, Special Publication 348: Geological Society, London. p. 87–114.

Roure F, Alzaga H, Callot JP, Ferket H, Granjeon D, Gonzalez GE, Guilhaumou N, Lopez M, Mougin P, Ortuño S, Séranne M. 2009. Long lasting interactions between tectonic loading, unroofing, post-rift thermal subsidence and sedimentary transfers along the Western margin of the Gulf of Mexico: Some insights from integrated quantitative studies. *Tectonophysics* 475:169–189.

Roure F, Swennen R, Schneider F, Faure JL, Ferket H, Guilhaumou N, Osadetz K, Robion P, Vandeginste V. 2005. Incidence and importance of tectonics and natural fluid migration on reservoir evolution in foreland fold-and-thrust belts. *Oil and Gas Science and Technology Review Institut Français du Pétrole* 60:67–106.

Salvador A. 1991. Origin and development of the Gulf of Mexico basin. *In* Salvador A (Editor). *The Gulf of Mexico Basin*, The Geology of North America, Vol. J: Geological Society of America, Boulder, Colorado. p. 389–444.

Sassi W, Rudkiewicz JL. 1999. THRUSPACK Version 6.2: 2D Integrated maturity studies in thrust areas. Institut Français du Pétrole Report 45372.

Sassi W, Rudkiewicz JL. 2000. Computer modelling of petroleum systems along regional cross-sections in foreland fold-and-thrust belts: EAGE (European Association of Geoscientists & Engineers) Conference Malta 2000, extended abstract.

Schneider F. 2003. Basin modeling in complex are: Examples from Eastern Venezuelan and Canadian foothills. *Oil and Gas Science and Technology Revue de l'Institut Français du Pétrole* 58(2):313–324.

Schneider F, Devoitine H, Faille I, Flauraud E, Willien F. 2002. Ceres2D: A numerical prototype for HC potential evaluation in complex area. *Oil and Gas Science and Technology Revue de l'Institut Français du Pétrole* 57(6):607–619.

Schneider F, Faille I, Flauraud E, Willien F. 2000. A 2D basin modeling tool for HC potential evaluation in complex area: 62nd EAGE (European Association of Geoscientists & Engineers); May 29–June 2; Glasgow (Abstract).

Schneider F, Pagel M, and Hernandez E. 2004. Basin modeling in complex area: Example from Eastern Venezuelan Foothills. *In* Swennen R, Roure F, Granath J (Editors). *Deformation, Fluid Flow and Reservoir Appraisal in Foreland Fold-and-Thrust Belts*, Hedberg Series, Memoir 1: American Association of Petroleum Geologists, Tulsa, Oklahoma. p. 357–369.

Tissot B. 1969. Premières données sur les mécanismes et la cinétique de la formation du pétrole dans les sédiments: Simulation d'un schéma réactionnel sur ordinateur. *Revue de l'Institut Français du Pétrole* 24:470–501.

Ungerer P. 1990. State of the art of research in kinetic modelling of oil formation and expulsion. *Organic Geochemistry* 16:1–25.

Ungerer P, Burrus J, Doligez B, Chénet PY, Bessis F. 1990. Basin evaluation by integrated two dimensional modelling of heat transfer, fluid flow, hydrocarbon generation and migration. *American Association of Petroleum Geologists* 74:309–335.

Ungerer P, Doligez B, Chenet PY, Burrus J, Bessis F, Lafargue E, Giroir G, Heum R, Eggen R. 1987. A 2D model of basin scale petroleum migration by two-phase fluid flow: Application to some case studies. *In* Doligez B (Editor). *Migration of hydrocarbons in sedimentary basins.* Editions Technip, Paris, France. p. 415–456.

Vázquez CE. 2004. Final report on "generator systems of the Basin Veracruz. Pemex Report (in Spanish).

Vázquez CE. 2008. The Veracruz gas province: Origin and distribution of the gas and petroleum perspectives [Master's thesis]: Instituto Politécnico Nacional, México, 138 p. (in Spanish).

APPENDIX.—Two-dimensional (2D) basin modeling in a complex setting: The CERES2D software specificities.

HISTORICAL PERSPECTIVE

Basin modeling aims at reconstructing the time evolution of a sedimentary basin in order to make quantitative predictions of geological phenomena leading to pressure generation and hydrocarbon accumulations. It accounts for porous medium deformation, heat transfer, hydrocarbon formation, and multiphasic fluid migration (e.g., Schneider et al. 2000).

Since the pioneer works on the modeling of hydrocarbon formation (Tissot 1969) have been available, several generations of basin model have been built. Initially, 1D models such as *Genex* were used to simulate the temperature evolution and the maturation of the organic matter. In the sedimentary basin context, the 1D approach is satisfactory for these purposes because the thermal transfers are mainly vertical. Indeed, thermal convective transfers are most frequently negligible. Then 2D model, such as *Temispack* (Chenet et al. 1986; Doligez 1987; Bessis et al. 1990; Ungerer 1990; Ungerer et al. 1987, 1990), were built. These 2D models provide the possibilities of performing an evaluation of the pressure history and appreciating hydrocarbon migration and reservoir filling. However, these evaluations are only qualitative because fluid (water, oil, and gas) migration is mainly convective and therefore sensitive to 3D geometry and anisotropy. For these reasons, a generation of 3D basin model was designed (e.g., *Temis3D*; Schneider et al. 2000).

The previous sedimentary basin models are able to handle relatively simple geometries resulting from deposition, erosion, and vertical compaction. However, since the exploration is now focusing in area such as foothills, a new generation of models able to handle faults was needed.

CERES2D BASIN MODEL

The CERES2D software used is the current study is composed of several modules managed by a study browser. The main modules include a section editor, a restoration module, and a forward simulation simulator. The other modules include a chronostratigraphy editor, a lithology editor, a kerogen editor, fluid editors, a mesh editor, a run editor, and visualization modules. The main steps required to conduct a case study are (1) the edition of the initial section, (2) the restoration of the section, and (3) the forward simulations.

Initial Section: The initial section is composed of a 2D cross section, which can be edited directly from scratch or can be imported from other software. At this stage, it is recommended that one use structural tools to balance the section. The geometry of the section is defined first. The geological attributes are then assigned, including horizons and faults labeling, decollement level definition, and finally the lithology distribution, which may evolve spatially but not in time.

At this stage, the blocks, which represent the smallest kinematics units, are defined and meshed with their own grids, with no constraint coming from the other blocks. The faults grids are created dynamically during the forward simulation. The initial section holds the upper mantle, the ductile lower crust, the brittle upper crust, and the considered sedimentary part.

Kinematic Scenario: Once the edition of the initial section is terminated, the past stages of the sections are created following a backward process, which includes kinematic restoration, backstripping, and thickness modification.

For each restoration scenario, the backward process is composed of different steps (Schneider et al. 2002). The first step is the editing of the eroded parts if erosion has occurred during the considered period. Importing templates may help with this edition. The second step is an automatic backstripping of the section. Once the erosion and the sedimentation have been accounted for, the resulting section is uncompacted using porosity–depth relationships. This section is then restored from a kinematics point of view. At this stage, the displacements along faults are accounted for, using translations, vertical shear, and/or flexural slip mechanisms.

The last step of the backward simulation requires the correction of local inconsistencies in the computed thicknesses, which result from the use of the vertical shear mode of deformation. This step allows accounting for salt or mud tectonics. Correction of the edition of the erosion may be done at this stage. These steps should be performed for each layer initially defined in the section at present day.

Forward Simulations: In these complex geometries, faults cut the basin into blocks that naturally define computational subdomains, using Domain Decomposition Methods (e.g., Faille et al. 1998). In each block, the model accounts for the porous medium compaction, erosion, heat transfer, hydrocarbon formation, and migration (Schneider et al. 2002, 2004; Schneider 2003). The equations are mass conservation of solid and fluids (water, oil, and gas) coupled with Darcy's law and a compaction law. The faults have a constant thickness, and their permeability may evolve with time. The prototype allows using three permeability models for the faults: Faults can either be assumed to be pervious (i.e., first option) or impervious (i.e., second option), at which point they are considered a flow barrier. Alternatively, their permeability can also evolve through time according to the neighboring lithologies (i.e., third option). Permeability can also change with the strain rate. Whichever option is chosen, the faults are considered to be inactive when their velocities are lower than the defined speed limit of 50 m/Ma.